Nanocarrier-Mediated Photochemotherapy and Photoradiotherapy

Denkova, Antonia G.; de Kruijff, Robine M.; Serra-Crespo, Pablo

DOI
10.1002/adhm.201701211

Publication date
2017

Published in
Advanced Healthcare Materials

Article type: review

Nano-carrier mediated photochemotherapy and photoradiotherapy

Antonia G. Denkova, Robine M. de Kruijff, Pablo Serra-Crespo*

Radiation Science and Technology, Delft University of Technology, Mekelweg 15, 2629 JB Delft, The Netherlands. *Email address: a.g.denkova@tudelft.nl

Abstract

Photothermal therapy (PTT) and photodynamic therapy (PDT) both utilize light to induce a therapeutic effect. These therapies are rapidly gaining importance due to the non-invasiveness of light and the limited adverse effect associated with these treatments. However, most pre-clinical studies show that complete elimination of tumours is rarely observed. Combining PDT and PTT with chemotherapy or radiotherapy can improve the therapeutic outcome and simultaneously decrease side effects of these conventional treatments. Nano-carriers can help to facilitate such a combined treatment. Here, the most recent advancements in the field of photochemotherapy and photoradiotherapy in which nano-carriers are employed are reviewed.

Keywords: combined phototherapies, chemotherapy, radiation therapy, nano-carriers

1. Introduction

Cancer is indisputably one of the main challenges in western healthcare, leading to more than 8.8 million deaths per year [1]. The top 5 cancer types contributing most to the morbidity numbers in order of decreasing occurrence are: lung, liver, colorectal, stomach and breast

cancer [2]. The choice of treatment depends on the cancer type, location and staging, but surgery is usually preferred followed by chemotherapy and radiotherapy. Each of these treatment options has its advantages but also restrictions, i.e. surgery is not always capable of removing all cancer cells or can even facilitate the spread of malignant cells while chemotherapy and radiotherapy (RT) can both have severe side effects due to healthy tissue toxicity and can induce resistance in cells. In this respect therapies relying on light are much more advantageous since they hardly cause any adverse effects, can be limited to the diseased site, provoke nearly no cell resistance and can be used as an external trigger for drug release [3]. However, these photo-based therapies are often not capable of complete tumour eradication and will greatly benefit from chemo- or radiotherapy, meanwhile reducing their adverse health effects. Combinational treatments are not a novel concept; nowadays chemotherapy and radiotherapy are often combined as it has been proven that the therapies are more effective when co-applied [4]. This is most likely due to the radiosensitizing abilities of the chemotherapeutics [5] as well as the possibility to attack metastasized cells. It is, however, not common practice to combine phototherapies with other therapeutic modalities and this is where nanotechnology can make a difference, providing numerous nano-systems with different functionalities [3b, 6].

This review will describe the essential requirements in the design of nano-carrier systems for combined photodynamic and photothermal therapy with chemotherapy or radiotherapy, focusing on the most recent developments in the field. Illustrative examples of each therapy combination will be provided and the paper will conclude with a clinical perspective. Figure 1 shows schematically an overview of this review.

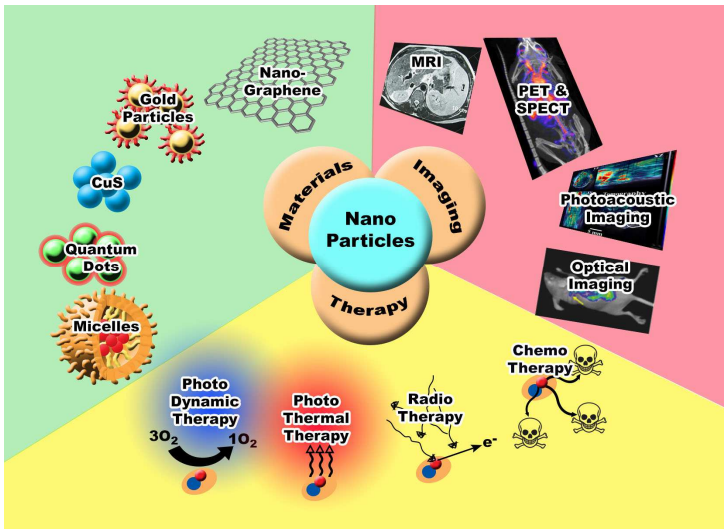

Figure 1 An overview of combined phototherapies mediated through nanoparticles and imaging possibilities

2 Different therapeutic modalities

2.1 Phototherapies: photothermal therapy & photodynamic therapy

Two types of phototherapies exist: photothermal and photodynamic therapy. While both need a photosensitizer (i.e. a molecule sensitive to photons), their working mechanism is rather different. Photothermal therapy (PTT) employs materials that when absorbing light, usually in the near-infrared (NIR) region as NIR is able to reach deeper situated tumours, produce heat and can thermally ablate tumour cells [7]. A good photothermal agent should have a strong absorbance of NIR, efficient transfer of the absorbed light into heat and no toxicity. In addition, the photosensitizer should accumulate in sufficient amounts at the tumour site preferably when systemically administered. This can be achieved if either the photothermal agent can function as a delivery system on its own or if it can be encapsulated in a nano-carrier. Examples include organic carriers often based on NIR-absorbing conjugated polymers [8] and different kinds of inorganic materials like gold [9] carbon [10], copper sulfide (CuS) [11].

An excellent review by Cheng et al. describes all the possible types of photothermal agents [6b]. Despite the clear potential of preclinical studies complete elimination of the tumour is often not observed due to the fact that heat is not homogenously distributed and it is not possible to have a temperature reading allowing readjustment of the treatment [12]. This is also probably the reason for the existence of just three clinical trials reported, two of which utilize the same nanoparticle. The nano-system in two of the clinical studies consists of PEGylated silica-cored Au nanoshells, known under the brand name AuroShell® particles [13]. The other clinically tested photothermal agent has also been composed of silica and gold and does not concern a cancer related treatment but cardiovascular therapy [14].

Photodynamic therapy (PDT) is used to generate singlet oxygen and other reactive oxygen species (ROS) from photosensitizers when exposed to light of certain wavelength. A photosensitizer (PS) gets activated by light to produce a short-lived excited singlet state which can either decay back to its ground state emitting fluorescence or form a relatively long-lived triplet state through intersystem crossing [15]. In PDT the triplet state is of importance since it can directly give its energy to a molecular oxygen, producing the highly reactive singlet oxygen which can damage cell organelles. Alternatively, the triplet state can interact directly with cells leading eventually to superoxide anion radicals, hydroxyl radicals and hydrogen peroxide, which in turn can induce cell damage. The particular wavelength depends on the absorbance of the photosensitizer, and the amount of singlet oxygen produced is related to the quantum yield. In the clinic, PDT is mainly applied to treat dermatological disorders, though more and more photosensitizers for cancer treatment are being developed. The most often used clinical photosensitizer is sold under the brand name Photofrin® and has been clinically approved for the treatment of obstructing esophageal cancer, obstructing lung cancer, gastric and papillary bladder cancer and cervical dysplasia [16]. Despite its potential PDT suffers from several limitations such as the need of an oxygen-rich environment, short tissue penetration

depth, lack of tumour selectivity and absence of accepted light dosimetry [3b]. Similarly to PTT inhomogeneous distribution of the photosensitizer may lead to areas that remain untreated preventing full destruction of the tumour. Furthermore, photosensitive molecules being often hydrophobic tend to aggregate, which can result in self-quenching and significantly decrease their effectiveness[17]. Nanotechnology can help to overcome a few of these problems. For instance, nano-carriers can help to bring highly hydrophobic photosensitizers to the tumour [18] and considerably reduce their aggregation by utilizing interactions between the photosensitizer and the carrier molecules (such as π-π stacking[19]), while up-conversion particles can increase depth penetration by converting light of a long wavelength to light of a short wavelength [20] increasing the applicability of PDT.

2.2. Chemotherapy

Chemotherapy employs cytotoxic drugs to attack fast proliferating cells. It is usually the first choice of treatment of metastases but it is also often given as adjunct therapy to reduce the risk of spreading the disease or the chance of reoccurrence. In addition, chemotherapy can be given to increase quality of life and overall survival of patients who cannot be cured. The main drawback of chemotherapy is that it also affects healthy cells that divide more frequently, such as cells in the digestive tracts and the bone marrow, which can result in side effects that depend on the drug of choice, the dosage, and the patient [21]. The effectiveness of chemotherapeutic drugs depends strongly on their pharmacokinetics and biodistribution, i.e. being often small molecules they can be excreted rapidly by the kidneys decreasing their tumour accumulation. Moreover, most of the available drugs are typically not very soluble in aqueous solutions, which limits the injected concentration, usually requiring several doses before an effect is observed. The success of a treatment strongly depends on the healthy tissue

toxicity versus tumour killing efficiency. While there is a large variety of chemotherapeutic drugs, doxorubicin (DOX), docetaxel (DTX), cisplatin (CDDP) and paclitaxel (PTX) are most common in drug delivery.

The potential of nano-carriers in chemotherapy has been well recognized and several formulations have been approved for clinical use [22]. The first nano-carrier to make it to the clinic is a liposome encapsulating DOX, which, since then has been accepted for several indications and marked as Doxil™/Caelyx™. It has been shown to be safer and equally efficient or even slightly better than the free drug [23]. Liposomes are currently the most widely applied nano-carrier, but polymeric micellar systems are gaining attention.

2.3. Radiation therapy

Radiation therapy is applied to approximately 7 million patients each year and is typically divided into external (beam) therapy, brachytherapy and radionuclide therapy. Radiation can lead to DNA (deoxyribonucleic acid) base damage, single strand breaks and double strand breaks, the last strongly depending on the radiation type. Direct DNA damage produced by high linear energy transfer (LET) radiation is more prone to induce double strand breaks which are more difficult to repair. However, most therapies use low LET radiation. Radionuclide therapy is a treatment usually applied to treat metastases and often utilizes a cancer cell targeting agent such as a peptide coupled to a beta particle emitting radionuclide [24]. Several examples of radionuclides used in radionuclide therapy are: ^{131}I ($t_{1/2}$= 8.04 d), ^{177}Lu ($t_{1/2}$= 6.7 d), ^{90}Y ($t_{1/2}$= 64 h), ^{64}Cu ($t_{1/2}$= 12.7 h) and ^{67}Cu ($t_{1/2}$= 67.1 h). In brachytherapy a radioactive source (usually ^{192}Ir, $t_{1/2}$= 73.8 d) is inserted in the close vicinity of the tumour or directly in it, delivering a high dose to malignant tissue which rapidly falls off sparing healthy tissue [25]. External beam therapy is a local treatment that can employ X-rays, gamma photons, electrons and heavier particles such as protons all aiming at damaging the genetic

material of cells. It is often also applied as palliative treatment. Oxygen dependence is one of the major drawbacks of most radio-therapeutic treatments since it limits their efficacy in hypoxic areas, which develop as the tumour grows. For combined applications mediated through nanoparticles, beam therapies using X-rays and gamma photons are the most relevant. In single therapy, the nanoparticles function primarily as radiosensitizers, enhancing the therapeutic effect of radiation [26]. The X-ray energy used in therapy varies from approximately 50 kV to 20 MV, but megavolt therapy is much more common because it can penetrate further into the tissue and reach more deeply situated tumours. The most advanced type of X-ray therapy is the so-called Intensity Modulated Radiation Therapy, which is able to deliver non-uniform dose distributions significantly diminishing damage to healthy tissue. Therapy is typically given in small fractions of 2 Gy (J/kg) per day for a period of time, depending on the cancer characteristics [27]. However, higher dose fractions are also delivered when gamma knife treatment is applied [28].

3. The role of nano-carries in combined treatments

Combined therapies often have a better therapeutic efficiency and diminished therapy resistance of the tumour cells built-up during treatment. In addition, when internal therapies are combined with external triggers systemic toxicity is reduced, as lower amounts of the chemotherapeutics need to be injected before an effect is observed. Nano-technology offers the possibility to design multi-functional carriers that facilitate combined therapies.

Nano-carriers are materials having nano-dimensions that are capable of transporting various drugs and imaging agents. These systems can be composed of metals[29], polymers[30], lipids[31], and non-metals such as silica[32] and graphene[33] and find applications in e.g. drug and gene delivery[34], photo- and radiosensitization[35], and imaging [36]. Some of these

formulations have made it to clinical trials. For instance, micelles composed of PEG (polyethylene glycol) and polyglutamate (PGlu) block copolymers conjugated with 7-ethyl-10-hydroxy-campothecin (SN-38) have been applied in the treatment of breast cancer [37]. The targeting mechanism of nano-entities relies on the enhanced permeability and retention (EPR) effect which is believed to occur when tumours reach certain size and force the formation of blood vessels which often appear to be leaky. The lack of lymphatic drainage in many tumours further enhances the accumulation of large substances. The EPR effect is often referred to as passive targeting in contrast to active targeting which utilizes targeting vectors such as peptides or antibodies to specifically target overexpressed tumour receptors. The existence of the EPR effect has been proven in many preclinical trials but whether it also occurs in the human body has been widely disputed. The heterogeneity of tumours, even when of the same type, is one of the reasons for these controversies. Factors such as tumour interstitial fluid pressure (IFP) and the degree of angiogenesis and lymphangiogenesis which may differ per tumour, will result in rather different outcomes [38]. Similar conflicting literature is found in relation to the active targeting of nanoparticles, as many groups report better tumour uptake when applying targeting entities but fail to explain these results [39]. Naturally, whether targeted or not a nano-carrier primarily relies on the EPR effect to reach the tumour [40]. Targeting may improve the retention at the tumour site as well as the cell internalisation and possible further diffusion, and is therefore still worth considering in particular applications.

Nano-carrier systems can serve as a platform for the combination of therapeutic modalities and imaging options. The main challenges that such nano-systems face are related to their pharmacokinetics, biodistribution and toxicity. For most applications, a sufficient amount of the nano-carriers needs to be accumulated at the tumour what requires a long blood circulation time. Furthermore, the majority of the nanoparticles will be taken up by the liver

and spleen and can become toxic over time if the body does not dispose them. Particularly in the field of drug delivery, additional challenges exist such as preventing drug release during circulation and controlled supply at the tumour site, since these are the main benefits of such a system vs. the free drug. Through combinational therapies some of these challenges can be solved. For instance it has been shown that radiotherapy can make malignant tissue more permeable which can lead to better tumour uptake [41]. Furthermore, triggered release allows for the design of 'loss-free' systems, which exhibit a much better release profile [42].

4.Photothermal therapy and chemotherapy

While photothermal therapy is usually insufficient to cause complete tumour eradication, combining it with chemotherapy can prove to be more effective than either therapy by itself. Nano-carriers are great platforms, which allow for easy incorporation of both therapies. We have divided the nano-carrier systems for photothermal therapy and chemotherapy into 4 categories: carbon materials, gold materials, other inorganic materials and organic materials, though there is some overlap between categories as some materials, like silica, are used in combination with various systems since they have mostly host-function. The general concept behind these systems is that the photothermal agent, whether it is main component of the carrier or not, should lead to an improved drug delivery rate of the chemotherapeutic optimizing the synergistic effect of the two.

4.1 Carbon materials

A variety of carbon materials (fullerenes, carbon dots, carbon nano-tubes (CNTs) etc.) have been designed for biomedical applications [43]. Among these, CNTs and nano-graphene exhibit the highest absorption of NIR light and are therefore considered excellent materials for photothermal therapy. However, in combinational treatments CNTs [44] have been less widely

studied and research has focused primarily on nanographene oxide (NGO) [45]. Just recently mesoporous carbons have made an appearance, though they have mainly been investigated in vitro and will not be further discussed in this review[46]

CNTs are divided into two types: single-walled (SWCNTs) and multi-walled carbon nanotubes (MWCNTs), and are characterized by their high aspect ratio which has been shown to lead to rather unexpected biodistribution effects and pharmacokinetics such as renal excretion [47]. CNTs, like other carbon materials, need to be functionalized in order to improve their solubility in aqueous media and enable attachment of targeting vectors and other entities. A recent example of a CNT system has been presented by Zhang et al. who have prepared quantum dots/DOX nanocomposites based on MWCNTs [44]. The CNT nanocomposites have shown to heat effectively and release the drug in the process, as well as to exhibit a pH responsiveness. Tumour killing efficiency has been tested upon intratumoural injection in A549 tumour-bearing nude mice, showing tumour inhibition for the combined treatment.

Nano-dimensioned graphene and graphene oxide were immediately recognised as excellent carriers for drug delivery being bio-inert materials with high loading efficiency which can be chemically functionalized [45a]. Furthermore, NGO has shown to be an excellent photothermal agent, absorbing NIR light when in its reduced form. In most cases an 808 nm NIR laser is applied for photo-activation while DOX is the drug of choice since its release is enhanced by a slightly acidic pH, additionally contributing to improved delivery in tumour cells. PEGylation of the graphene particles is usually desired to increase circulation time, enhancing tumour uptake and drug delivery. Although most studies rely on the EPR-effect for tumour uptake, in some cases targeting agents have been applied such as in the study by Dong et al. [45b]. They have used transferrin coated NGO to cross the blood brain barrier and attack glioblastoma tumours. Although no quantitative data on tumour uptake has been given the results have shown that when chemotherapy is combined with photothermal heating mediated

by the carrier, the survival is significantly improved as compared to non-targeted NGOs. This indicates that transferrin has facilitated the transport of particles through the blood-brain barrier (BBB). A rather different approach has been followed by Song et al. who have prepared vesicles encapsulating graphene and DOX coated by golden nano-rods instead of targeting agents [45c]. This system has a much better photothermal activity than just gold and/or graphene. The improved photothermal behaviour has been ascribed to the plasmonic coupling of the golden rods conjugated on the vesicle-surface and the interaction of the NGO with the plasmonic coating. Furthermore, it has been shown that the DOX is released upon photoheating, thus providing means of triggered drug release. Very promising tumour inhibition and overall survival (i.e. 100 % survival in 40 days) have been found in U87MG tumour bearing mice upon single intravenous injection, heated with a NIR laser (808 nm). Combining NGO with gold has also been investigated by Chen et al. [45d] who have prepared dual-therapy particles. In this case, however, an additional conducting polymer (polyaniline, PANI) has been employed which has tremendously improved the photothermal behaviour of the composite (Figure 2). Assembled gold nanoparticle (AuNP) core polyaniline shell particles have been added to polyvinylpyrrolidone-stabilized graphene oxide, after which the high surface area of graphene has been exploited for DOX loading. DOX release has been shown to be greatly enhanced when the nano-composite is exposed to a NIR laser (808 nm) and at the same time the cell killing efficiency has been determined to be much higher when PANI had been introduced to the particles. The in vivo results have shown that the nano-composites with and without DOX have been able to achieve total tumour elimination in 4T1 xenografted mice models, but the DOX containing nanoparticles have realized faster tumour-volume reduction.

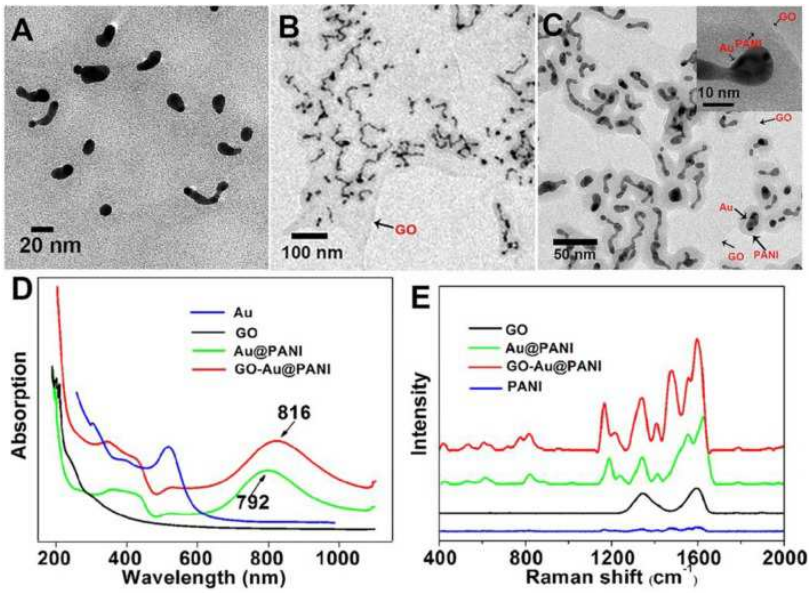

Figure 2 The TEM images of Au@PANI A) and GO-Au@PANI with different resolutions B) and C), the UV-vis-NIR absorbance spectra D) and the Raman spectra of the nanostructures E). Reproduced with permission from ref. [45d]. Copyright 2016 Ivyspring International Publisher.

4.2 Gold based materials

Nano-dimensioned gold has been applied as a platform for various biomedical applications due to its biocompatibility and the possibility to synthesise a versatile library of nano-structures. Many of the applications of gold in biomedicine take advantage of the optical phenomenon called localised surface plasmon resonance (LSPR). Due to this optical characteristic, the light absorbance of gold particles can be shifted to the desired wavelength. Gold nanoparticles usually have two LSPR different emission modes, one originating from the transverse mode (around 520 nm) and one from the longitudinal, the position that depends on the aspect ratio and can be shifted in the NIR region [48]. Particularly in the field of phototherapy light absorption around 800 nm is desired because of deeper tissue penetration. Part of the absorbed energy is dissipated into heat, which is utilized in photothermal therapy. Different structures and compositions can be found in the literature to facilitate combined

phototherapy and chemotherapy [49].

Mesoporous silica as a coating is one of the preferred platforms as it allows for high drug loading and can easily be functionalized with targeting agents or PEG [50]. Wang et al. have deviated from the commonly used spherical shape and prepared nano-rods composed of gold nanoparticles and mesoporous silica relying on previous reports showing that elongated particles are more efficient in cell killing [50f]. The authors have studied three different aspect ratios and in all cases DTX has been encapsulated in the PEGylated silica matrix. The small, medium and large rods (l x w: 125 x 95 nm, 207 x 105 nm and 385 x 155 nm respectively) have been studied in vitro, where medium rods had the best uptake. The therapeutic effect has been evaluated through intravenous injection in mice with highly aggressive melanoma tumours, where all aspect ratios have shown good therapeutic potential though only the medium sized rods eliminated tumour reoccurrence. Cheng et al. have also used gold nanoparticles in combination with mesoporous silica, but in this case the gold nanoparticles have been used as gate keepers of the chemotherapeutic drugs [50d]. Gold capping has been shown to not only reduce the DOX release but actually enable controlled drug release, as discharge is almost immediate upon NIR irradiation which nearly stops when the laser is switched off, allowing for repetitive drug supply. The biodistribution of these particles has been determined in vivo by conjugating DOTA (1,4,7,10-tetraazacyclododecane-1,4,7,10-tetraacetic acid) to the particles and chelating it with the PET (positron emission tomography) isotope ^{64}Cu, revealing good tumour uptake. Unfortunately, no therapeutic studies have been reported thus far.

Polymer-based coatings have been widely applied to cover gold nanostructures and provide means for drug encapsulation and the introduction of other functionalities [39a, 51]. An emerging nature-inspired polymer is polydopamine (PDA) which has gained tremendous interest due to its various different functional groups allowing the implementation of several

functionalities. This polymer has been utilized by Zhang et al. who have coated small gold nano-rods with PDA to prepare particles for combined therapies and SPECT (single photon emission computed tomography) imaging [39a]. In this particular case, the particles have been PEGylated and the RGD (arginine-glycine-aspartic acid) peptide has been conjugated to the surface. Cisplatin has been added to the PDA surface possibly by the coordination of [Pt(H2O)2(NH2)2]2+ with 5,6-dihydroxyl groups in catechol (Figure 3). In addition, the PDA surface allowed for chelator-free Iodine (^{125}I) labelling which has facilitated preclinical SPECT imaging. Cisplatin has been demonstrated to be released at low pH as desired, while the ^{125}I labelling remained intact. RGD targeting has shown to lead to higher tumour uptake and the therapeutic studies in lung carcinoma tumours have revealed that the best results are obtained when both treatments are combined. Photothermal therapy by itself led to relapse of the tumour.

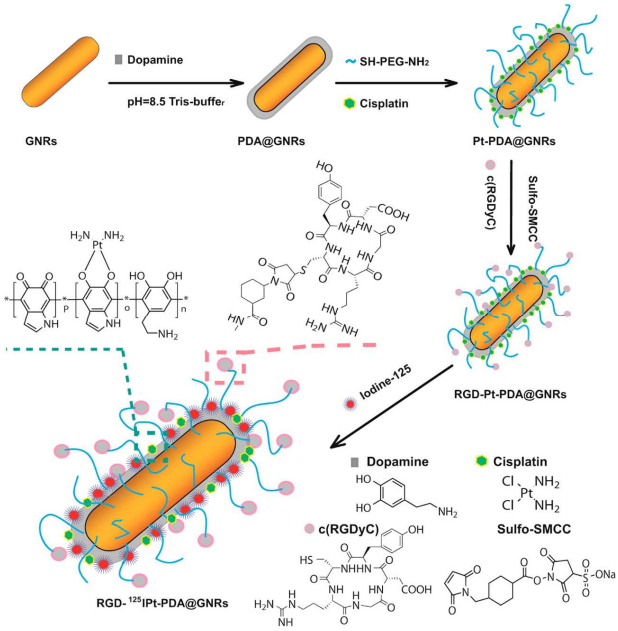

Figure 3 A schematic overview of the synthesis of gold rods coated with PDA. Reproduced with permission from reference [39a]. Copyright 2016 American Chemical Society.

A rather different approach has been proposed by Zheng et al. [51d] who has applied a

liposome co-assembled with a pH and thermo-responsive polymer to serve as gate keeper of a chemotherapeutic drug encapsulated in porous golden particles. The polymer, poly(N-isopropylacrylamide–methacrylic acid–1,4-dioxane, octadecyl acrylate) (p(NIPAM-MAA-ODA)), has served as the dual responsive macromolecule. The surface of the liposomes has been further functionalized with aptamers for tumour targeting. The idea behind this design has been that upon NIR laser irradiation a temperature increase is induced which causes phase transitions of the NIPAM and forces the phospholipid chains to stand perpendicularly as to open the gate. At the same time, the low pH changes the confirmation of the polymer also leading to release of the drug. In vitro studies have confirmed the enhanced release of a model drug (DOX) at low pH and upon NIR irradiation. The therapeutic studies have shown that combined treatment with DOX-containing nanoparticles and NIR irradiation gave superior results than any of the individual treatments. Most importantly, these experiments have indicated that sufficient amounts of the chemotherapeutic drug can reach the tumour site to induce a synergistic effect, which is often the downside of such constructs when administered systemically.

4.3 Other inorganic materials

There are numerous inorganic nano-systems besides gold that have been proposed for combined photothermal- and chemotherapy, but taking into account the most recent studies three main groups can be identified: PTT agents enclosed in porous silica, Prussian blue (PB) and CuS based systems. Unlike PB and CuS, silica itself has not been utilized as a photothermal agent but simply as a carrier allowing high loading due to its high surface area and easy functionalization due to its robustness. A large variety of silica coated systems designed for combined photo- and chemotherapy can be found in the literature, even in combination with PB or CuS [52]. A nice illustration of the advantages of silica is the work by

Zhao et al. who have developed small silica-polymer hybrids of approximately 30 nm, which high porosity and pore volume has been utilized to carry the photothermal agent palladium phthalocyanine and PTX [53]. The release of PTX has found to be higher at higher temperatures, probably due to faster diffusion, which could nicely be combined with the photo-thermal activation of the palladium compound. Good tumour uptake has been observed upon intravenous injection, and although liver uptake has been the most pronounced it has been found to decrease within a few days. Therapeutic evaluation in a sarcoma xenografted mouse model has revealed that the particles have good anti-cancer potential even when not loaded with PTX, although the best survival and no re-occurrence has only been observed for the combined treatment. A different porous silica morphology has been prepared by Deng et al., who have conjugated the photothermal agent cypate to silica nano-tubes encapsulating DOX [54]. Here, the narrow pores of the silica have forced the cypate to aggregate in a J-type which has resulted in much better photo-activation as compared to the free photosensitizer. This enhanced photothermal activity in combination with DOX has shown complete tumour elimination in 4T1 tumour bearing mice upon intravenous administration. The authors have also demonstrated that the nano-carriers are able to deliver higher amounts of cypate to the tumour than the free administration of the photothermal agent which explains the excellent therapeutic outcome of the study.

PB is a dark blue pigment known from ancient times which consists of mixed-valence transition metal hexacyanoferrates. This dye has been proven to have a very strong absorbance in the NIR region and has been approved by the FDA for clinical use which consequently has resulted in the synthesis of various structures and combinations [55]. The combination of chemotherapy and phototherapy has been demonstrated by Tian et al. who have covered PB particles by a mesoporous silica layer enclosing DOX [55e]. The silica has been further modified to contain thiol groups to which Cy-5.5 (cyanine-5.5) has been

conjugated for optical imaging. The particles have been tested in vivo through intravenous injection, not only focussing on the therapy but also on the magnetic resonance imaging (MRI) possibilities of PB. MRI capabilities have been confirmed and the therapeutic evaluation has shown beneficial effects of the combined treatment. However, complete regression of the tumour has not been observed, which is most likely due to lower tumour uptake compared to studies where intratumoural administration has been carried out. A way to improve tumour uptake has been suggested by Chen et al. who have designed hollow porous PB nanoparticles covered by a red blood cell (RBC) membrane for simultaneous delivery of DOX and phototherapy (Figure 4) [55d]. The red blood cell membrane has been applied to mislead the immune system thereby increasing blood circulation time and achieving a better biodistribution. A common problem of nano-carriers is their fast clearance from the body and accumulation in organs such as the liver and spleen which prevents sufficient tumour uptake. With this approach the authors have tried to mislead the body's immune system and increase blood circulation. The in vivo studies have proven this idea to be successful as 14 % of the nanoparticles have been still found in the blood circulation after 24 hours which is more than twice as much as the uncoated particles. This higher accumulation together with the high loading efficiency of DOX and the NIR stimulated release have led to 98 % tumour inhibition in mice bearing 4T1 tumours.

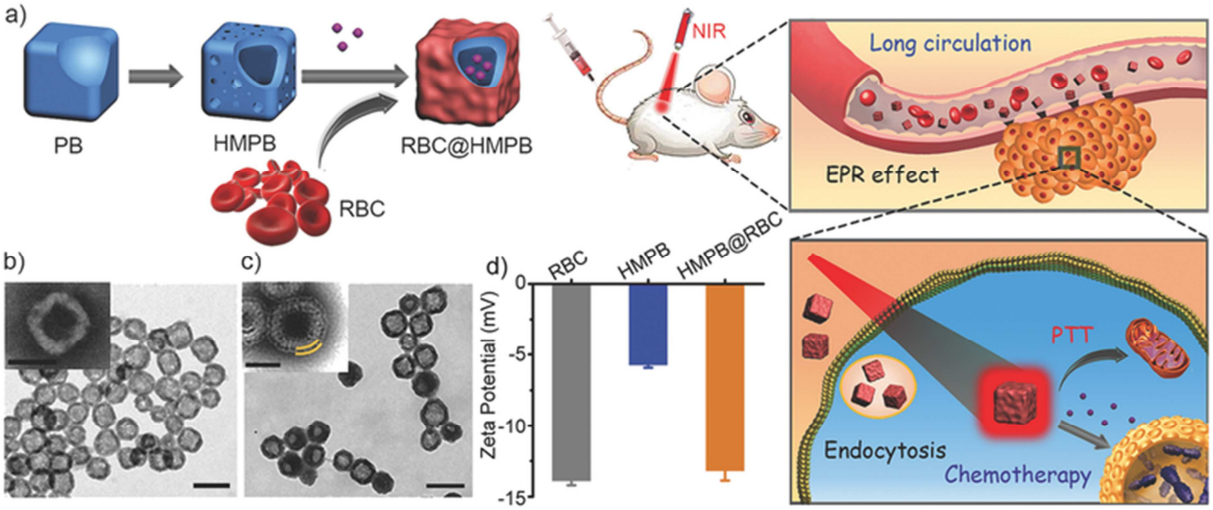

Figure 4 A) Illustration of the preparation of drug loaded PB particles covered by RBC and the synergistic photothermal-/chemotherapy of cancer. TEM images of B) PB NPs and C) PB@RBC NPs (scale bar = 100 nm). Inset: high magnification images of the nNPs, with potassium phosphotungstate staining (scale bar = 100 nm). D) Surface charge of RBC vesicles, PB NPs, and PB@RBC NPs.

CuS has been widely investigated in phototherapy in various dimensions and interesting nano-structures such as flowers due to its low cost and wide range of NIR absorption [52b, 56]. Their NIR absorption arises from d-d intra-band transitions of Cu^{2+} ions, with transition peaks at ~900 nm. Unlike gold-based materials, where the NIR absorption stems from LSPR, the absorption wavelength in CuS nanoparticles is not influenced by the surrounding environment or nanoparticle size or shape, resulting in a better thermal stability and higher photothermal conversion efficiency [57]. Before it can be successfully applied in the preclinical setting, the CuS surface needs to be modified to reduce cytotoxicity and improve biocompatibility, and should be designed as a platform for drug delivery next to photothermal heating. This has been demonstrated by Wang et al. who have synthetized ultra-small CuS particles (d = 3.5 nm) conjugated to poly-acrylic acid (PAA) [56d]. These conjugates have been loaded with DOX by electrostatic interaction and eventually covered by poly(allylamine hydrochloride)

(PAH) to minimize DOX release. The particles have been tested intratumourally in a 4T1 murine model showing complete removal of tumour. An interesting prodrug combination based on Pt (platinum) and CuS have been reported by Bi et al. [56c]. In this study small CuS particles have been conjugated to the cisplatin based prodrug (Pt IV) which can be reduced producing the cytotoxic Pt(II) ions when internalized in the cell and in the presence of glutathione (GSH). The particles have been PEGylated and functionalized with folic acid for improved tumour accumulation leading to Pt amounts at the tumour site above 10 μg per gram of tumour. The combination of the CuS prodrug particles and NIR have given the best tumour killing efficiency revealing a positive synergistic effect.

4.4 Organic particles

Although inorganic particles often exhibit superior absorption of NIR light, they are in most cases not degradable and can accumulate in different healthy organs, causing inflammations even if they are not toxic [58]. In this respect, organic particles are much more advantageous as they are usually biocompatible, degradable and can be more easily modified to facilitate combined treatments [30]. The majority of the organic nano-systems are used as carriers of photothermal dyes and chemotherapeutic entities [59-60]. A good example is a combination of the liposome, a well-known and clinically accepted system, with a photothermal agent as investigated by Yan et al. In this work temperature-sensitive liposomes have been loaded with IR-780 in the lipid bilayer and DOX in the aqueous cavity [61]. The idea behind this design has been to use NIR lasers to excite the IR-780 and produce heat which will force the temperature sensitive liposomes to release the drug. The therapeutic efficacy has been investigated in mice having mammary carcinoma xenografted tumours. Upon release of the drug from the liposomes using the NIR laser the tumour has been completely eliminated in 100 % of the

tested animals. Important to mention is that the liposomes were injected intravenously and can therefore be used for the treatment of a variety of tumours exhibiting the EPR effect. Su et al. have prepared polymer-based amphiphilic systems in the form of micelles composed of methoxy polyethylene glycol (mPEG) and poly(D,L-lactideco-glycolide) (PLGA) conjugated to porphyrin [62]. It has to be mentioned that although the authors refer to micelles, the transmission electron microscope (TEM) images and the ability of the particles to encapsulate both the hydrophilic drug (DOX) and the hydrophobic drug (PTX) indicate that the nano-assemblies are, in fact, vesicles. The nano-carriers have been shown to heat up upon laser irradiation due to the porphyrin, which resulted in somewhat enhanced release of both drugs. Intravenous injection has been used in the therapeutic studies, demonstrating much more pronounced tumour reduction or even complete elimination of the combined treatment with no adverse side effects (Figure 5).

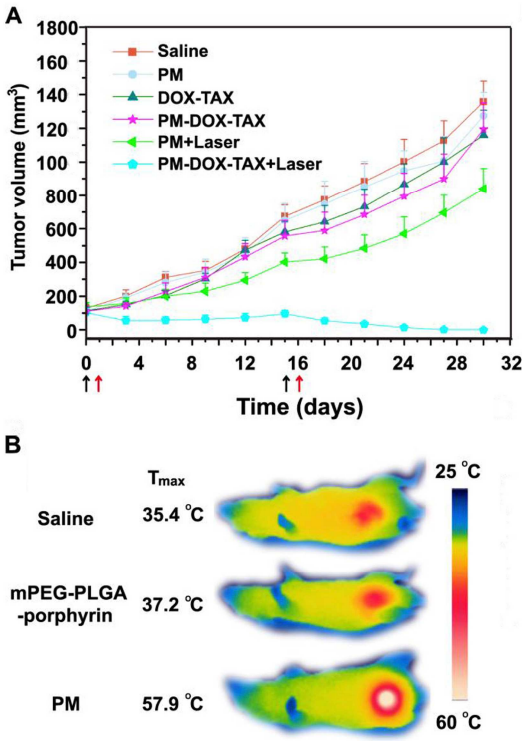

Figure 5 *In vivo* antitumor effects of DOX–TAX-loaded porphyrin micelles and photothermal efficiency of porphyrin micelles. (A) Antitumor efficacy of various drug formulations in an

orthotopic triple-negative breast cancer model in BALB/c nude mice. Mice bearing MDA-MB-231 tumors (~100mm^3) were treated with different formulations (n = 5/treatment group). The treatment schedule was indicated by black arrows for intravenous injection of drugs and red arrows for the laser irradiation. PM, porphyrin self-assembled micelle; PM–DOX–TAX, PM simultaneously loaded with DOX and TAX. (B) Infrared thermo-graphic maps of tumors after near-infrared laser irradiation for 8 min. Adapted with permission from reference [62]. Copyright 2016 Elsevier.

5. Photothermal therapy and radiotherapy

The combination of photothermal therapy and radiotherapy is relatively new, however, the number of publications is steadily increasing. The main advantage in combining these two treatment options is the PTT driven possibility to induce intratumoural hyperthermia which can increase the blood flow in tumour cells, improving oxygenation and subsequently causing the cells to be more sensitive to radiation [63]. Nano-materials used for this combination present high NIR absorbance and can produce a very localized increase in temperature while having a radiosensitizing effect. They are composed of inorganic materials commonly based on copper sulphides [64], quantum dots [65], or gold [66] or bismuth [67] containing compounds. In the following section the application of these materials has been divided into PTT combined with either external radiotherapy or (internal) radionuclide therapy.

5.1 PTT and external radiotherapy

Gold is a well-known photothermal agent as described in section 4.2, but also a radiosensitizer capable of producing photo- and Auger-electrons [68] and therefore a very logical choice for this combined therapy. One of the first studies in this field has been published by Diagaradjane et al. who have prepared gold nano-shells consisting of a 120 nm silica core surrounded by a 12-15 nm gold coating [69]. In vivo studies have been performed by intravenously injecting the gold nanoparticles in mice inoculated with human colorectal cancer cells (HCT 116). NIR irradiation has been combined with X-ray therapy using a 125 kV X-ray given in a single 10 Gy dose, resulting in a more than twofold increase of the tumour doubling time when compared with the single therapies. Gold-nanospikes have been developed by Ma et al. having a 50 nm diameter and excellent stability in PBS (phosphate buffered saline) [66]. In vitro tests have revealed that cell survival is greatly reduced when phototherapy is combined with 6 MV X-rays, and have led to in vivo studies in which the benefit of the combinational treatment has been evident resulting in pronounced tumour reduction in comparison to the individual treatments. Unfortunately, the in vivo studies have been based on intratumoural injection, and it is therefore not evident if the particles will perform well upon intravenous administration, with sufficient tumour uptake and low toxicity to healthy organs, to be able to serve as anti-tumour agents. A similar approach has been followed by Liu et al. who have designed Au nanoparticles having Pt spikes which they called nanodendrites [70]. The addition of Pt to the gold entities resulted in a broadening of the absorption spectrum of the particles, allowing excitation with NIR light. Cell viability has been determined upon NIR irradiation in combination with X-rays, yielding a higher killing efficiency than simply based on additive results. No in vivo studies have been reported for this study.

Bismuth-based nanoparticles, having comparable properties as gold, have also made an appearance in this combined therapy. The first proof of radiosensitization due to Bi has been

demonstrated only recently by Yu et al., who have applied ultra-small (3.6 nm) PEGylated bismuth nanoparticles labelled with a cyclic peptide (CGNKRTRGC, LyP-1) for enhanced tumour uptake and retention (Figure 6) [67]. This peptide specifically targets p32 proteins expressed by 4T1 murine breast cancer cells. A 1.7-fold increase in tumour retention has been observed for the targeted nanoparticles and complete tumour eradication has only been obtained for the combined therapy, leading to significant cell apoptosis and angiogenesis suppression in the tumour. Similarly, Du et al. have designed Cu_3BiS_3 nanocrystals which have been functionalized with amphiphilic D-α-tocopherol PEG 1000 succinate (TPGS) for improved stability [71]. The nanoparticles have shown complete tumour growth inhibition upon intratumoural injection only for the combined PTT and RT. The presence of copper in the particles has allowed for catalysation of two reactions; the reaction of endogenic H_2O_2 inside the tumour microenvironment as well as O_2•− generated from photoelectrons via the copper-catalysed Haber–Weiss reaction to yield highly reactive HO•, which has increased the level of oxygen radicals further destroying the cancer cells.

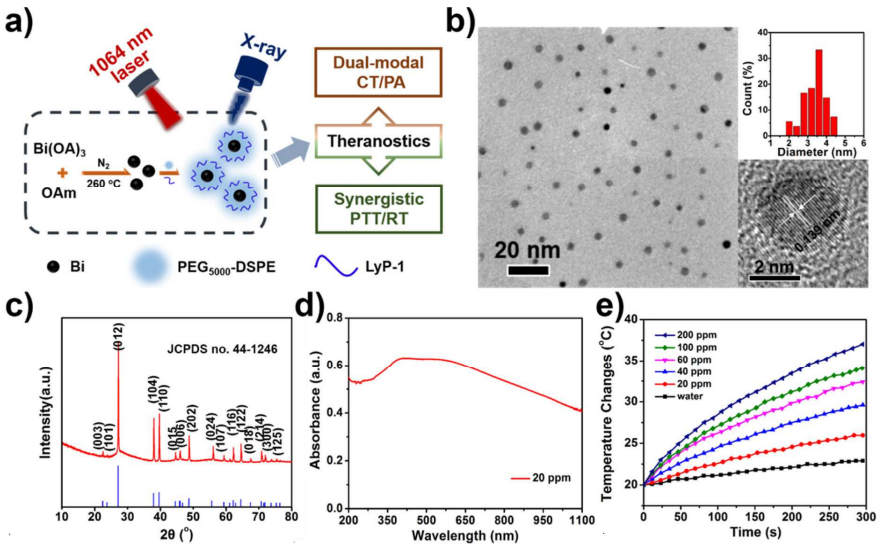

Figure 6 Scheme and characterization. (a) Scheme of multifunctional Bi NPs. (b) TEM images and HRTEM images of as-synthesized Bi NPs. Inset histogram shows the measured diameters of as-synthesized Bi NPs. (c) XRD pattern of as-synthesized Bi NPs. (d)

Absorbance spectrum of PEGylated Bi NPs. (e) Temperature changes of PEGylated Bi NPs at different concentrations under a 5 min irradiation from a 1064 nm laser at 1W cm^{-2}. Reproduced with permission from reference [67] . Copyright 2017 American Chemical Society.

Quantum dots (QDs) are mostly known for their fluorescent properties due to their high quantum yield and have been applied in biomedicine as non-invasive imaging agents [72]. Still, part of the absorbed energy of quantum dots is converted to heat which makes them potential photothermal agents. QDs often contain heavy metals and can therefore also exhibit a radiosensitizing effect. The potential of these particles in combined PTT and RT has been demonstrated by Young et al. who have prepared 3 nm WS_2 QDs [65] and tested them in vivo through intratumoural administration. The WS_2 QDs have exhibited good biocompatibility, good X-ray computed tomography (CT) and photoacoustic imaging (PAI) capabilities, and the combined therapy has shown a remarkable synergy in the eradication of the tumour. Intravenous administration of QDs has been tested by Wang et al. who have synthesised MoS_2 quantum dots covered with polyaniline [73]. Despite the size increase by the addition of polyaniline, their circulation half-life has been improved from 0.85 h (bare MoS_2) to 5.02 h (MoS_2@polyaniline) facilitating better tumour accumulation. Furthermore, the in vivo results have shown enhanced tumour reduction when combining the treatments. However, no biodistribution data has been given and it is therefore not clear whether uptake in healthy organs might be an issue. It needs to be mentioned that the particle toxicity has been studied in murine breast tumour cells as well as human umbilical vein endothelial cells revealing minor toxic effects.

5.2 PTT and (internal) radionuclide therapy

CuS is the most often applied nanoparticle in internal radionuclide therapy combined with PTT, prepared either by directly substituting a few of the Cu atoms for the radioisotope ^{64}Cu or by adding an additional radiolabel. A series of publications of the same group have appeared in which [^{64}Cu]CuS nanoparticles have been proposed as platform for simultaneous photothermal, radiotherapy, and PET imaging [64, 74]. ^{64}Cu, a great theranostic radionuclide which decays via positron emission, beta minus decay and electron capture, has been applied as a structural component of the nanoparticles. In vivo studies in different tumour models (breast, glioblastoma and thyroid) have been performed, showing no systemic toxic effects and good tumour reduction. PET imaging has further allowed for quantification of the biodistribution and subsequent dose calculations [74].

Yi et al. have used a different approach in utilizing the same type of nanoparticles, i.e. they have doped them with ^{131}I for combined image-guided PTT and RT treatment of primary and metastatic tumours [75]. ^{131}I has been incorporated in the NPs during synthesis, after which they have been PEGylated and tested in vitro with 4T1 murine breast cancer cells. Subsequent in vivo experiments have been carried out in the same tumour model, monitoring both the primary tumour and lymph nodes. The nano-particles have been shown to migrate to the lymph nodes which, if also exposed to NIR, could help to prevent metastases. Figure 7 demonstrates how the combined treatment has decreased the tumour volume offering an evident synergistic effect, where in all other treatment options the tumour volume has continued to increase.

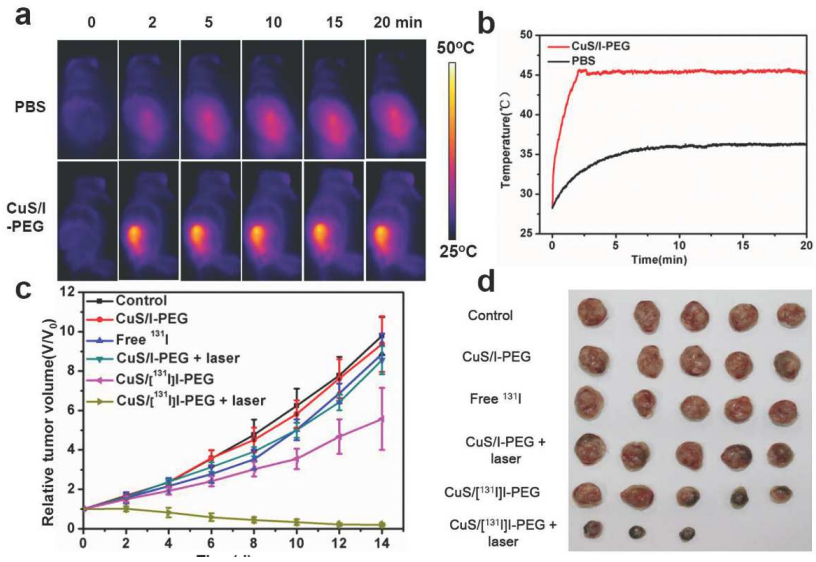

Figure 7 In vivo combined internal RT and PTT for treatment of subcutaneous tumours. A) IR imaging of mice injected with CuS/I-PEG or PBS under the 808 nm laser irradiation at 0.25 W cm^{-2} for 20 min. B) The temperature changes of the tumour based on IR thermal imaging date in (A). C) Tumour growth curves of mice with various treatments including PBS control, free ^{131}I injection, CuS/I-PEG injection without or with laser irradiation, as well as CuS/[^{131}I]I-PEG injection without or with laser irradiation. D) Representative photos of tumours collected from mice at day 14 after different treatments.

Other examples of internal RT combined with PTT include different metal nanosheets. For instance, Cheng et al. have decorated Bi_2Se_3 nanosheets with $FeSe_2$ nanoparticles labelled with ^{64}Cu [76]. The Bi_2Se_3 nanosheets have been formed by the addition of $Bi(NO_3)_3$ to pre-made $FeSe_2$ nanoparticles via cation exchange, after which they have been functionalized with PEG. The composite material has been labelled with ^{64}Cu without the need of any additional chelating agent. Due to the properties of the different elements present, it has been possible to perform multimodal imaging including MRI, CT, PAI and PET. In vivo experiments have been carried out in 4T1 tumour-bearing mice upon intravenous injection, showing the combined therapy to be superior to the treatments delivered separately.

6 Photodynamic therapy and chemotherapy

Nano-carriers have been widely investigated in the combination of photodynamic therapy and chemotherapy and can function as carriers or energy converters. It needs to be emphasised that many photo-responsive systems exist which are used for triggered drug release. However, in this review only particles taking advantage of PDT are reviewed. These systems are divided into three main groups; up-conversion particles, silica particles and organic particles.

6.1 Up-conversion particles

Up-conversion nanoparticles (UCNPs) are materials that are able to convert light of low energy (high wavelength) to light of high energy (low wavelength) due to anti-Stokes emission. UCNPs that find application in photo-chemotherapy widely vary synthetically but often consist of a ceramic material serving as the host doped with transition- or rare-earth metals, such as Yb^{3+}, Ti^{4+}, Er^{3+}, etc. $NaYF_4$ is the most commonly applied host although many materials classify as hosts as long as their crystal structure and cationic size do not influence the conversion process and allow for sufficient doping [77]. The dopant ions are the actual energy converters and their type and concentration will influence the conversion efficiency. Typically at least two kinds of dopants are necessary, a sensitizer (e.g. Yb^{3+}) and activator (e.g. Er^{3+}) [78]. Up-conversion particles usually have an additional coating to which the photosensitizer and the chemotherapeutic drug are either adsorbed or conjugated.

Dong et al. have encapsulated DOX, inorganic UCNP and Zn-Phtalocyanine (Zn-PCN) in bovine serum albumin−poly(ε-caprolactone) block copolymers which have also been modified to contain folic acid (FA) for targeting purposes [79]. This resulted in two types of self-assembled structures, one with and another without FA. The up-conversion nanoparticles have served to convert near-infra red light of 980 nm to visible light and activate the Zn-PCN

to produce ROS particles of a size range between 40 to 53 nm depending on the amount of encapsulated photosensitizer. The presence of folic acid has improved cell uptake as expected but it had hardly any influence on the performance of the irradiated particles as compared to the ones having no targeting moiety. However, in both cases the combination of chemotherapeutic drug and photodynamic therapy have resulted in much better tumour cell killing efficiency. In vivo studies have not been performed as of yet. In somewhat similar approach Yang et al. have synthesised UCNP doped with Mn^{2+} ions as MRI contrast agent [20]. The particles have been covered with mesoporous silica in which a photosensitizer could be stored. Leakage has been prevented through the use of composites with an amphiphilic copolymer having 9,10-di-alkoxyanthracene groups. The authors have proposed that the amphiphilic polymer forms micelles in which the UCNP can be encapsulated resulting in core-shell particles (Figure 8). In this formulation DOX (or similar drugs) can also be loaded during the self-assembly. Chlorin e6 has been excited by NIR light, which has been converted to match the spectrum of the photosensitizer. The singlet oxygen produced by chlorin e6 has subsequently been used to break the amphiphilic polymer and release the drug. The nano-composites have also been tested intratumourally, where a positive effect has been found for both the DOX containing as well as the drug-free particles.

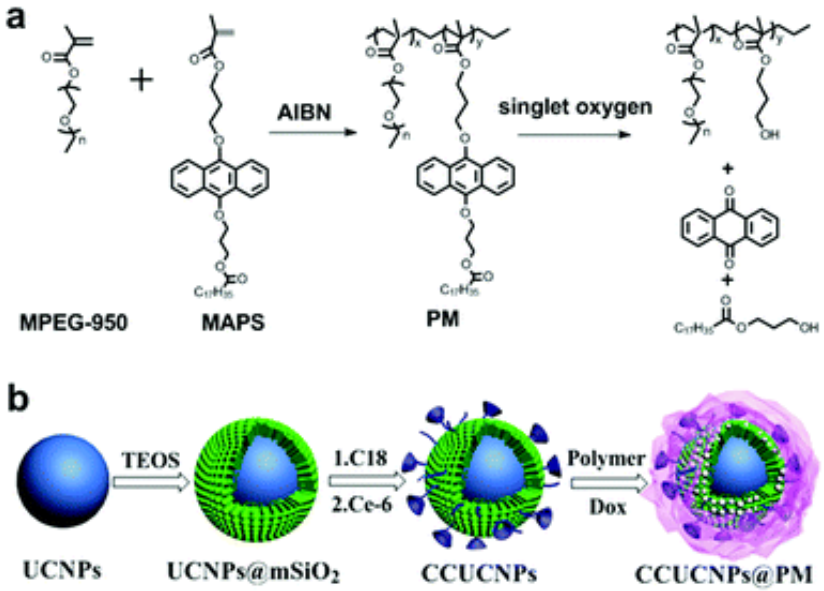

Figure 8: Schematic illustration of (a) the synthesis of PM and the degradation under singlet oxygen; (b) the preparation of CCUCNPs@PM. Reproduced from reference [20]. Copyright 2014 RSC.

A complete investigation of UCNPs has been carried out by Wang et al. who have synthetized NaYF4:Yb/Er engulfed in DSPE-PEG (1,2-distearoyl-sn-glycero-3-phosphoethanolamine-polyethylene glycol) to improve solubility [80]. DOX has been conjugated to PEG through a singlet oxygen-sensitive linkage (a thioketal linkage) and the photosensitizer merocyanine 540 (MC540) has been added in the formulation. The idea behind this design is to use the UCNPs to convert 980 nm light into 540 nm photons which excite the photosensitizer, which in turn produces singlet oxygen resulting in the cleavage of the thioketals and the release of DOX. The results demonstrate good DOX release upon illumination and subsequently enhanced tumour reduction in in vivo experiments. Moreover, the authors have shown that folic acid conjugated UCNPs gave the best results demonstrating that targeting can be beneficial, contrary to recent opinions on the benefit of targeting [40].

6.2 Silica based particles

High surface area silica is the preferred choice as host material due to its versatility, biocompatibility and the possibility to encapsulate or conjugate high amounts of drugs and photosensitizers. This has been demonstrated by Zhang et al. who have employed mesoporous silica particles to simultaneously encapsulate chlorine e6 and function as a platform for the conjugation of cisplatin [81]. The authors have investigated their system only in vitro indicating that at high concentrations of cisplatin there is no additive effect of PDT but at lower amounts the combined therapy has yielded more potent anti-cancer activity. Yang et al. have investigated the effect of the mesoporous silica particles' shape in the delivery of DOX and chlorin e6 [82]. For this purpose chlorine e6 has been conjugated to the silica compound, which has been employed along with the tetraethyl orthosilicate (TEOS) in the preparation of the inorganic particles. The amount of chlorin e6 has influenced the shape of the particles going from spherical to ellipsoid and eventually to rods, where the rod-shaped particles exhibited the highest tumour uptake. DOX has also been loaded into the particles and has been released at a pH of 5.5, most likely due to the protonation of the amino groups of the drug. The particles have not exhibited any toxicity in the dark. These particles have been intratumourally administered in mice and the influence of laser irradiation as well as the presence of DOX has been examined, again proving the benefit of combined treatment. Unfortunately no in vivo data of intravenously injected particles has been presented, making it difficult to properly assess the potential of these carriers for tumours that are not easily accessible. Mesoporous hollow silica particles have been further investigated as carriers for fullerenes (C-60) and DOX [83]. For this purpose, a selective etching method has been used to produce hollow particles of around 50 nm containing C-60 in their shell and allowing for the encapsulation of drugs in the cavity. The fullerenes have been used as photosensitizers allowing both chemotherapeutic treatment as well as PDT, which indeed have shown the best tumour cell killing efficiency when compared to single treatments using the same carriers.

Yao et al. has also investigated silica particles for drug release and PDT [84]. In this paper, PEGylated tetraphenylporphyrin zinc (Zn-POR-CA-PEG) has been used as gate-keeper to lock to pores of the mesoporous silica particles and limit the release of encapsulated chemo-drugs. For this purpose the silica has been modified with histidine facilitating an interaction with the Zn-Por-CA-PEG, which is pH sensitive and leads to the release of both the porphyrin as well as the chemotherapeutic drug. Similar to the other studies the combined treatment induced the highest cytotoxicity.

6.3 Organic nano-carriers

A variety of different organic nano-materials have been synthesised and tested. These organic platforms can either just act as a carrier for the photosensitizer and the drug or be composed of the photo-reactive substance itself [18b, 39b, 85]. A few examples of each system will be discussed below.

6.3.1 Self-assemblies composed of photosensitizers

One of the most simple and yet efficient self-assembling systems of photosensitizers has been developed by Zhang et al. who have self-assembled DOX with the photosensitizer chlorin e6 based on electrostatic interactions, π-π stacking and hydrophobic forces [18b]. The size of the self-assemblies has depended on the ratio of the two compounds, allowing for the preparation of small 70 nm particles, which under dialysis have exhibited a delayed release of DOX and chlorine e6 as compared to the pure compounds. In cell cultures the combination of chemotherapy and photodynamic therapy has been less evident in contrast to the in vivo studies where the joint therapy has led to total elimination of the tumour. The increased effect in vivo can be ascribed to the better tumour accumulation of the NPs in comparison to free

chlorin e6, which has been found to be eliminated from the animals in less than 12 hours. The fate of DOX in vivo could not be followed but the biodistribution is likely similar to that of chlorin e6. In subsequent studies, the same group has improved the particles by conjugating DOX to PEG via a Schiff base bond, introducing a pH response to the system. The tumour penetrating peptide arginylglycylaspartic acid (RGD) has also been attached for improved tumour targeting [85b]. The in vivo results have revealed better tumour uptake and drug retention than the original particles and consequently superior therapy response. A somewhat similar approach has been followed by Zhang et al. who have prepared supramolecular self-assemblies of the platinum(IV) prodrug bridged b-CD dimer and a porphyrin photosensitizer [39b]. The size of these aggregates has been around 100 nm and they have been utilized to deliver both compounds very efficiently to cells, especially in comparison to CDDP or its prodrug. Interestingly, neither the prodrug nor the photosensitizer had a large cytotoxicity under the absorption of light when applied on their own. However, when combined they reduced the IC50 values of Pt by almost 15 times compared to cisplatin controls.

Analogously Chen et al. have modified human serum albumin (HSA) to either conjugate chlorin e6 or RGD [86]. Subsequently, they have used the mixture of both conjugates to encapsulate PTX or first enclose PTX in the HSA-chlorin e6 assemblies before adding the HSA-RGD. Although the self-assemblies have differed in size they have exhibited similar pharmacokinetics and biodistribution when administered intravenously. The therapeutic efficiency of the first self-assembly has been evaluated and indicated very good tumour response, especially when compared to controls not containing RGD, due to the lower tumour uptake of the latter. Interestingly, the authors have also explored the ability of chlorin e6 to chelate Mn^{2+} ions, introducing MRI capabilities

A series of publications has been dedicated to the design of metal containing supramolecular nanogels (SNG) based on porphyrins for the delivery of chemotherapeutic drugs [87]. Yao et

al. have examined the in vivo potential of one of these systems, the self-assembled dextran-g-histidine (DH) copolymers with tetraphenylporphyrin zinc (Zn-Por) for combined PDT and chemotherapy. pH responsiveness of this system is provided by the histidine, which binds to Zn-Por at neutral pH while at higher acidity it gets protonated initiating the dissociation of the SNG. The size of the 'self-assemblies' has been shown to depend on the concentration of Zn-Por. Both dextran-g-histidine self-assemblies and the SNGs have been loaded with DOX. While the loading efficiency of the SNGs is not very high, they have a favourable release profile showing less than 20 % loss at neutral pH and more than 80 % at a pH of 5.3. Subsequent in vivo studies have demonstrated that the SNGs loaded with DOX had the same tumour reduction potential as free DOX, but when irradiated with wavelengths ranging from 400 to 700 nm the SNG loaded with DOX outperformed all controls including the SNG without the drug, clearly indicating that combined chemotherapy and PDT is more effective. Wang et al. have also explored supramolecular complexes consisting of histidine and iron-tetraphenylporphyrins (Fe-TPP) to prepare micelles which have served to transport a chemotherapeutic drug [88]. Here, again pH responsiveness has been observed which facilitated drug release at acidic pH. The effectiveness of this system has unfortunately only been verified in in vitro studies.

6.3.2 Organic systems as carriers

A variety of organic materials such as liposomes [89], block copolymer micelles [90], lipid particles [91] have been tested as vehicles. The advantages of liposomes as compared to other systems are their ability to deliver hydrophilic and hydrophobic substances [92] [92-93], as well as the fact that they have clinical acceptance. However, the large variety of building blocks of polymer and lipid-based micelles allows for fine tuning of their size and composition which

can also serve to reach much higher loading efficiencies than liposomes. An advantage of all carriers is that in principle they can be utilized in the field of photochemical internalisation (PCI) and improve the effectivity of biotherapeutic drugs tremendously [94]. It is well known that the largest obstacle in efficient delivery of biotherapeutics is overcoming the barrier of endocytic vesicles engulfing foreign entities[94b] [95]. The general working principle of PCI is the uptake of the photosensitizer in the endo-lysosomes, preferably in the membrane, which upon light excitation produces singlet oxygen that can destroy the organelles, freeing the imprisoned molecules or carriers [96]. PCI mediated by nano-carriers is especially relevant for the delivery of large molecules such as in gene therapy. Here on the one hand the encapsulation of biomolecules in nano-carriers improves their cellular uptake while photochemical destruction of the endosomes allows for their escape. A nice example of such a system is the work by Pasparakis et al. who have prepared a block copolymer composed of polyacetal and polyethylene oxide although in this case somewhat smaller molecule has been used as a model drug [90b]. The polyacetal unit can be triggered by both protons and light as shown in Figure 9, which allows for drug release when exposed to either ultraviolet/visible photolysis at single photon (365 nm), double photon (532 nm), and even multi-photon (1,064 nm) excitation, as well as at slightly acidic pH of approximately 5.2. These block-copolymer self-assembles into roughly 190 nm diameter nanoparticles which can encapsulate a hydrophobic drug of choice. Camptothecin (CPT) has been chosen as a model drug and its release and cytotoxicity in combination with hematoporphyrin (HP) has been investigated under different conditions such as laser irradiation using either a continuous wave or pulses. The type of laser irradiation has influenced the therapeutic potential of the nanoparticles, where a pulsed laser has resulted in an increased killing efficiency. As a possible mechanism, the authors have proposed that the NPs disintegrate once located in the endosomes due to both the local low pH as well as laser irradiation. The HP can further damage the endosomal

membrane due to the production of ROS upon irradiation and subsequently result in the release of CPT. Remarkably, when both drugs are used without being encapsulated in the micelles, the cytotoxicity is much less pronounced. This might be due to a different cellular fate, indicating the added value of the carrier.

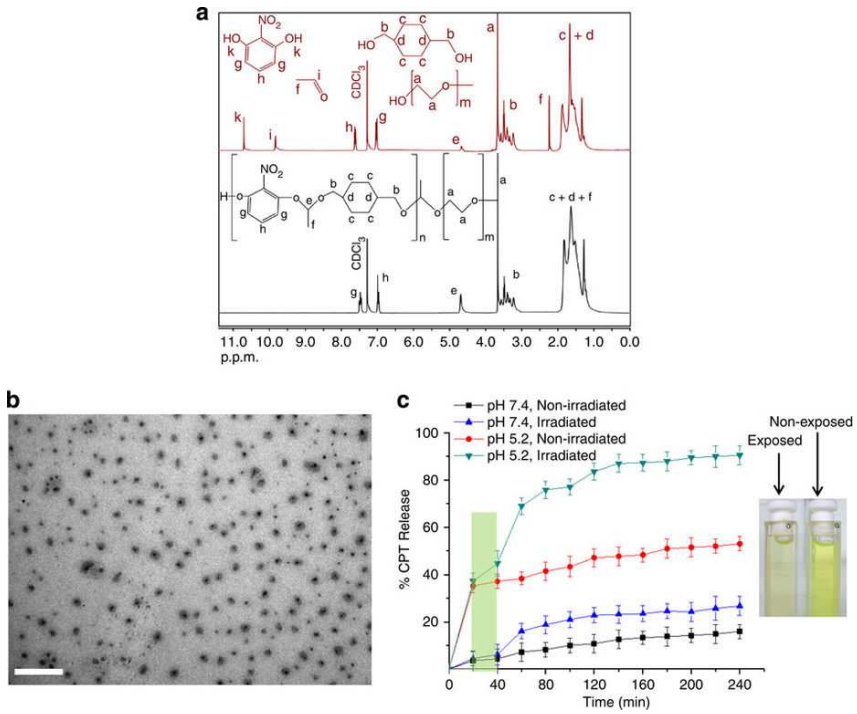

Figure 9 A) ^{1}H NMR spectra of the initial polymer solution in d-chloroform (non-exposed) (in black) with the corresponding spectrum (in red) of the laser-irradiated sample showing characteristic diminution of the acetal proton (peak e) and the appearance of acetaldehyde (peaks i and f) and 2-nitroresorcinol (peak k) protons, B) TEM microphotograph of polyacetal nanoparticles and C) % CPT release from NPs at different pH and laser irradiation conditions (the green stripe represents the irradiation interval), and digital photograph of laser-exposed and non-exposed polymer solution. Scale bar, 500 nm. Reproduced from reference [90b]. Copyright 2014 Nature Publishing Group.

Their biocompatibility and versatile loading capabilities make liposomes ideal agents for

combined photodynamic- and chemotherapy. Recently, Wang et al. have demonstrated the encapsulation of PTX and the photosensitizer sinoporphyrin sodium (DVDMS) in liposomes for the treatment of a MCF-7 (breast cancer) xenografted model [89a]. In vitro studies have shown that the dual-loaded liposomes mainly accumulate in the cytoplasm. The ROS produced upon laser irradiation have caused mitochondrial dysfunction and thus have sensitized cell apoptosis by PTX, showing again how two different therapeutic modalities can enhance one another. The pharmacokinetics and biodistribution of the vesicles have been found to be similar to normal liposome systems, where maximum tumour uptake has been achieved 12 hours after administration at which time laser irradiation has been applied. As expected the best tumour reduction has been observed for the combined PTX/DVDMS treatment with no significant side effects. However, it needs to be mentioned that the tumour has not been entirely destroyed probably due to the fairly low PTX concentration.

Besides PCI, organic carriers are used to induce cell death in various other ways. A particularly innovative approach has been suggested by Wang et al. who have developed lipid-PLGA particles coupled to RGD to co-deliver the photosensitizer indocyanine green (ICG) and the hypoxia-activated prodrug tirapazamine (TPZ) to tumour cells [97]. The idea behind this construct is that the photosensitizer consumes the oxygen present in the cells which can trigger the action of TPZ. 3D spheroidal tumour cell studies have first been carried out. They have shown a two-fold increase in uptake as compared to non-targeted particles and suggested that upon illumination (and subsequent ROS generation) the TPZ effect is more pronounced. Targeting the carriers with RGD has been shown to result in the best tumour-to-liver ratio, though also a somewhat higher kidney uptake. Therapeutic experiments have compared RGD conjugated particles containing only the photosensitizer or the hypoxia-activated drug with those carrying both entities. Remarkably, even upon simultaneous injection of the nanoparticles containing either TPZ or ICG, they still have not managed to

compete with the dual-loaded carriers, which have led to almost complete elimination of the orthotopic tumour. Similar tactics have been followed by Chen et al. who have also encapsulated TPZ in organic-inorganic composites [98]. TPZ has been first added to mesoporous silica, on which layers of per-O-methyl-b-cyclo-dextrin-grafted-hyaluronic acid (HA-CD) and tetraphenyl porphine tetrasulfonic acid (TPPS4) have been accumulated using layer-by-layer deposition resulting in supramolecular assembled photosensitizers (SupraPS) which have served to protect the TPZ from leaving the particles. In addition, Gd ions have been added to the TPPS4 to allow for MR imaging. The particles appear to target the CD44 receptor of cancer cells and respond to hyaluronidase (HAase), which is up-regulated in tumours and can release TPZ and supraPS from the particles (Figure 10). The particles have exhibited a remarkably good tumour uptake and tumour growth reduction compared to controls not containing TPZ or not exposed to infra-red light to trigger the production of singlet oxygen.

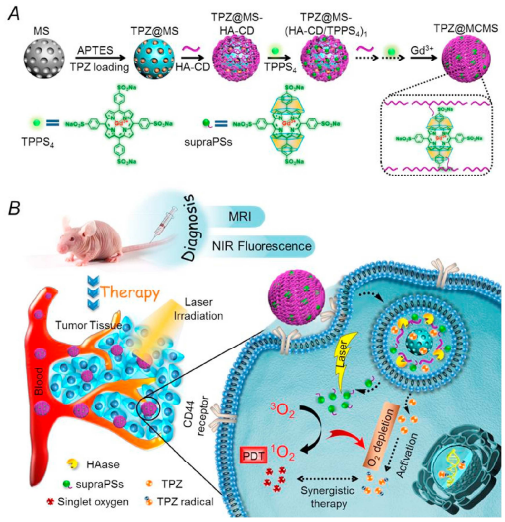

Figure 10 A) Layer-by-layer assembly of HA-CD and TPPS4 on TPZ loaded MSN to prepare the theranostic nano-platform B) Schematic illustration of tumour-targeted versatile theranostic nano-platform to achieve superior antitumor efficacy by the collaboration of

supraPSs-based photodynamic therapy and bio-reductive chemotherapy. Reproduced with permission from reference [98]. Copyright 2017 Elsevier.

A different strategy of using organic vehicles is the study of He et al. who have developed assemblies composed of nano-scale coordination polymers (NCP) designed to evoke an anti-tumour response by combining chemotherapy with PDT [99]. These NCP particles have been utilized to carry the chemotherapeutic drug oxaliplatin and the photosensitizer pyrolipid. Oxaliplatin itself has been used to form the core of the particles and has been covered with a monolayer of 1,2-dioleoyl-sn-glycero-3-phosphate (DOPA) and pyrolipid based on hydrophobic interactions. The outer lipid layer also contained PEG to reduce interactions with the mononuclear phagocyte system (MPS) and increase blood circulation when administered intravenously. The drug release has been found to be favourably decreased when the NCP has been protected by the pyrolipid. Although the in vitro studies have not shown an additional immunogenic response when pyrolipid is co-applied, the in vivo results have clearly indicated that the immune system has been stimulated. Tumour growth-regression of the primary tumours and, more importantly, decrease in distant (metastasised) tumours in two bilateral syngeneic mouse models of colorectal cancer have been demonstrated as clear evidence of an immune response. The same group has also investigated these particles loaded with cisplatin, but in this case only focussed on the synergy of photodynamic therapy and chemotherapy in a human head and neck cancer (SQ20B) xenograft mouse model [52a]. The best tumour reduction has been obtained upon irradiation here as well, when both cisplatin and pyrolipid are present.

7. Photodynamic therapy and radiotherapy

Photodynamic therapy combination with radiotherapy is a rather new field and the number of publications is still limited, but fast growing [18a, 100]. The main rationale behind this combination is based on the ability of wide-band materials to transform X-rays into light photons in the UV/VIS region. The ionizing radiation interacts with these scintillators through the photo-electric or Compton effect depending on the X-ray energy and the Z of the material, creating in the process many electron-hole pairs. Luminescence occurs when the hole and the electron are consecutively trapped at the luminescence centre and recombine. The produced luminescent light is then used to activate a photosensitizer and produce singlet oxygen. The first demonstration of this concept has been carried out by Chen et al. who have applied a rare-earth based nano-scintillator [100c]. Rare-earth materials are the preferred choice for the realization of this concept since they have excellent stopping power and produce good photon yields depending on their structural defects [100a, 100d, 100e, 100g, 101]. However, other metals such as Zn [100f], non-metal based scintillators [102] and even quantum dots [103] have also been studied. In all approaches the photosensitizer can either be encapsulated in a coating combined with the scintillator or conjugated directly on the particles. For instance, Clement et al. have used small CeF_3 particles (d = 9 ± 2 nm) as scintillator conjugated with the photosensitizer verteporfin [100d]. This study has revealed singlet oxygen production when irradiated with 8 KeV X-rays. The experimental results have been used to calculate the singlet oxygen production when using both the typical therapeutic beams of 6 MeV X-ray energy as well as the 30 keV used in brachytherapy. As expected, lower X-ray energies have yielded better results as the photons deposit more of their energy into the nanoparticles. Nevertheless, significant cytotoxicity has been reported in cell viability studies even when using 6 MeV beams although the effect is relatively low (32 %). Several other rare-earth nano-scintillators have been investigated in vivo. Chen et al., for instance, have developed $SrAl_2O_4:Eu^{2+}$ nanoparticles which they have coated with solid silica followed by a mesoporous silica layer

[100b]. The solid silica simply acts to protect the inorganic scintillator, while the mesoporous silica has facilitated the loading of the photosensitizer merocyanine 540 (MC540). After showing that the scintillator is capable of converting the X-rays into light, which via the photosensitizer produces singlet oxygen, the authors have carried out a therapeutic study based on intratumoural injection. The tumour shrinkage of the nanoparticles has been several times better than the controls showing without a doubt the co-action of the scintillator and the MC540. Zhang et al. used a similar approach but instead of a typical photosensitizer they have employed a semi-conductor to generate ROS [18a]. They first prepared octahedral Ce(III)-doped $LiYF_4$ seeds which they covered with silica functionalized with thiol groups which in turn have been used to encapsulate ultrafine ZnO nanoparticles. The in vivo studies have shown that tumours upon injection of nanoparticles and exposure to 8 Gy radiation exhibited near complete tumour growth inhibition.

From the non-rare earth metal-based materials, the so-called afterglow particles composed of copper and cobalt co-doped ZnS (ZnS:Cu,Co) conjugated to the photosensitizer tetrabromorhodamine-123 (TBrRh123) need to be mentioned [100f]. This study has investigated both singlet oxygen production upon X-ray exposure as well as cytotoxicity effects comparing X-ray treated and non-treated cells. The long after-glow of the particles has provided a more efficient light source for PDT after X-ray therapy revealing a significant difference in cell viability when radiation was applied in the presence of the nanoparticles.

Non-metal based converters are much less common and no in vivo studies have been reported so far. A nice example in this category is the study by Rossi et al., who have shown highly reduced cell survival as compared to controls when exposing their particles in lung cancer cells to 2 Gy radiation at a therapeutically relevant X-ray energy (6 MV) [102]. Their particles consist of SiC/SiO_x core-shell nano-wires conjugated with tetra(N-propynyl-4-aminocarbonylphenyl)porphyrin (H2TPACPP).

Although nearly all studies use rare-earth elements or metals for the conversion of X-rays to light, there are also those who report a synergistic effect based on combined radio- and photosensitization. In this respect the work of Liu et al. needs recognition as it reports the intravenous injection of PEGylated nanometric metal-organic frameworks (NMOF) composed of Hafnium (Hf^{4+}) and tetrakis (4-carboxyphenyl) porphyrin (TCPP). The Hf ions interact with X-rays and produce photons and Auger electrons which can serve as radiosensitizers in external beam therapy, while TCPP is a photosensitzer producing singlet oxygen upon light exposure [104]. The synthesised particles had a somewhat wide dispersity with an average diameter of 130 nm. After promising in vitro results their behaviour has been further investigated in vivo focusing on toxicity issues and biodistribution. The particles have been found to have good tumour uptake and typical high retention in organs of the MPS (i.e. liver and spleen), which, however, strongly decreased in 30 days showing that the particles do not remain in the healthy organs and therefore are not expected to cause inflammation. Subsequently, their tumour killing efficacy has been tested in breast tumour models applying X-rays, laser irradiation at 661 nm, or both. X-ray treatment has been found to have better tumour reduction than laser irradiation, but the combined treatment has clearly given the best results (Figure 11).

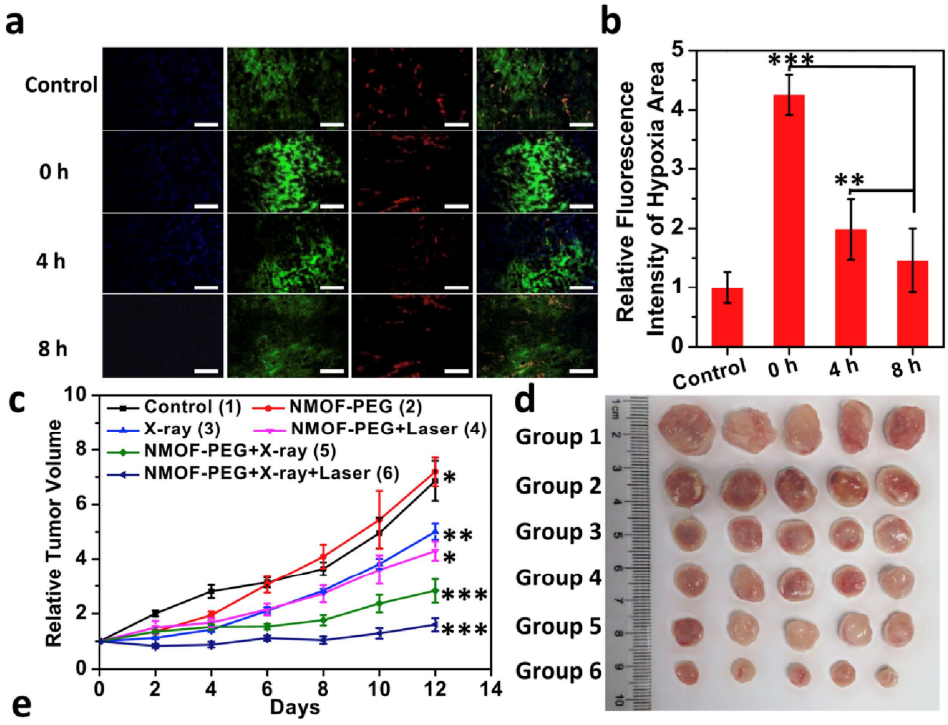

Figure 11: In vivo combination therapy. (a) Representative immunofluorescence images of tumor slices at different time post RT. The nuclei, blood vessels and hypoxia areas were stained with DAPI (blue), anti-CD31 antibody (red), and anti-pimonidazole antibody (green), respectively. The scale bar: 150 μm.(b) The relative fluorescence intensity of hypoxia are as recorded from more than 10 micrographs for each group. (c) Tumor growth curves of different groups after various treatments indicated: (i) untreated control, (ii) i.v. injection with NMOF-PEG, (iii) X-ray irradiation, (iv) i.v. injection with NMOF-PEG + Laser, (v) i.v. injection with NMOF-PEG+X-ray, (vi) i.v. injection with NMOF-PEG+X-ray+Laser. Error bars were based on SD of five mice per group. P values were calculated by Tukey's post-test (***$p < 0.001$, **$p < 0.01$, or *$p < 0.05$).(d)Photograph of tumors from mice after receiving various treatments collected at day 14. Reproduced with permission from [104]. Copyright 2016 Elsevier.

8 Imaging advantages

Molecular imaging is used to non-invasively obtain information about biological processes at the molecular level. It is applied in disease detection and staging, as well as monitoring the response to treatment. The role of molecular imaging in PTT and PDT mediated by nano-carriers is primarily associated with the biodistribution of the nano-entities, including pharmacokinetics and ex-vivo analysis. In such applications, it is imperative that the imaging probe is strongly bound to the nano-carrier or, even better, if the nanoparticle is the actual imaging entity. Photoacoustic imaging (PAI) is typically linked to PTT, while optical imaging is commonly associated with both PTT and PDT due to the often inherent fluorescence of the nano-carriers. In some reports the addition of an MRI contrast agent or a PET or SPECT radionuclide are mentioned. A few examples of each will be reviewed below.

PAI has gained tremendous popularity in biomedicine in the last decade due to its high spatial resolution (up to 5 μm) and relatively long penetration depth (a few centimetres) in tissue [105]. The main principle behind this technique is the absorption of NIR laser light by a suitable absorber, inducing heat formation and in turn causing thermo-elastic expansion and subsequent generation of mechanical pressure waves at ultrasonic frequencies. This combined optical and ultrasound imaging takes advantage of the high contrast of the first and the high spatial resolution of the second. Photoacoustic imaging requires a strong NIR light absorber at the imaging site as well as a pressure transducer close to the tissue to detect the outgoing waves. As discussed in section 4, there are a variety of inorganic particles (e.g. gold, PB, CuS etc) and organic nano-entities, either containing small dye molecules or being composed of semiconducting polymers which absorb NIR light and can in principle be used in PAI. A recent example of PAI combined with PTT triggered drug delivery are the DOX-loaded golden nano-shells developed by Lee et al. [106]. In this study, the authors have explored the possibility to use the inherent fluorescence of DOX to follow the drug release with optical imaging, and at the same time used PAI to monitor temperature increase upon photothermal

heating. The nanoshells have been injected both intravenously as well as intratumourally, where it was found that the fluorescence intensity considerably increased upon laser heating indicating drug release. The photoacoustic images have confirmed in vivo temperature increase of more than 20 % upon laser irradiation. PAI has also been used in biodistribution studies as demonstrated by Yao et al. (Figure 12). [107]. These authors have synthesised NIR absorbing amphiphilic polymers which self-assemble into micelles that can encapsulate chemotherapeutic drugs such as DOX. This study very nicely illustrates how PAI can be quantitatively used to determine the biodistribution of nanoparticles without the need of an additional contrast agent.

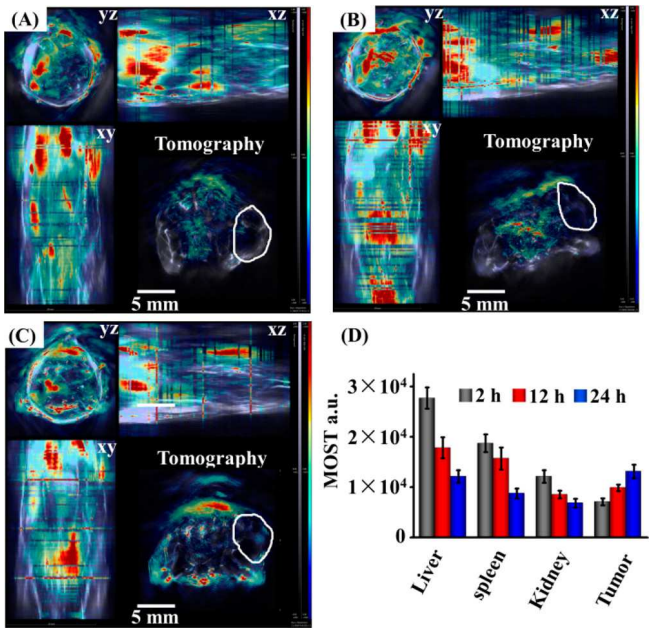

Figure 12 PAI of tumour-bearing mice treated with DOX-NPs after (A) 2, (B) 12 and (C) 24 h; (D) quantitative analysis results from PAI of DOX-NPs accumulated in liver, spleen, kidney, and tumour at different times. Reproduced with permission from reference [107]. Copyright 2014 American Chemical Society.

Optical imaging includes both bioluminescence and fluorescence imaging, the difference being that the first relies on living organisms' emission of light while the second requires a

light excitable probe. It is an indispensable technique in preclinical studies since it has a very high sensitivity, needing only concentrations in the pico molar range of an optical probe and allowing combined bioluminescent and fluorescent studies. The major drawback of this technique is its penetration ability, limiting its clinical application to surface or intra-operative applications [108]. In PDT and PTT therapy a NIR agent is often used which can serve as both a therapeutic and optical imaging agent [109] though in some cases an additional probe is added. Naturally, a double-acting probe is preferred since its inherent properties are not disturbed by the addition of agents which otherwise may influence physico-chemical characteristics such as nano-carrier charge and size. This has been demonstrated by Liu et al. who have synthesised a nanoscale zirconium-porphyrin metal–organic framework (NPMOF) encapsulating DOX [110]. The embedded porphyrin molecules served as both fluorescent imaging agent and singlet oxygen generator. Optical imaging has been applied to determine the pharmacokinetics and biodistribution of the nanoparticles (Figure 13), as well as optimize the moment of laser activation of the porphyrin providing an image-guided treatment.

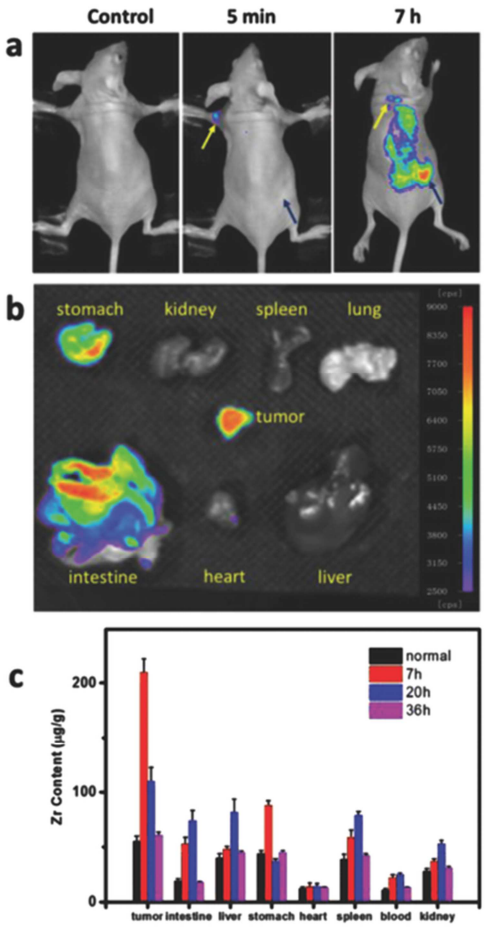

Figure 13 Fluorescent imaging of tumour-bearing mice administrated with NPMOFs A) NPMOFs have quickly accumulated in small lymph node (yellow arrow) at 5 min and in subcutaneous transplantable tumour (blue arrow) after 7 h through EPR effect. B) Fluorescent imaging of dissected organs of cancer-bearing mouse. C) Biodistribution of NPMOFs in main organs of mice (tumour, intestine, liver, stomach, heart, spleen, blood, and kidney).

MRI is a widely accepted technique in the clinic, especially suitable for obtaining information on soft tissue, capable of delivering anatomical as well as physiological information. It uses strong magnetic fields, radio waves, and field gradients to produce imaging data of organs. MRI contrast agents are not always necessary but commonly applied in tumour imaging. In the reported studies of combined photo-therapies MRI is less frequently applied. Nevertheless, a few examples demonstrate that MRI can aid in tumour identification and guide photo-based therapies. For instance, Wang et al. have synthesised a magnetic graphene-

based mesoporous silica platform loaded with DOX [111]. The embedded Fe_3O_4 nanoparticles have both served as MRI contrast agent and provided magnetic targeting properties. Figure 14 shows that MRI contrast is enhanced when magnetic targeting is applied, although this was not quantitatively evaluated.

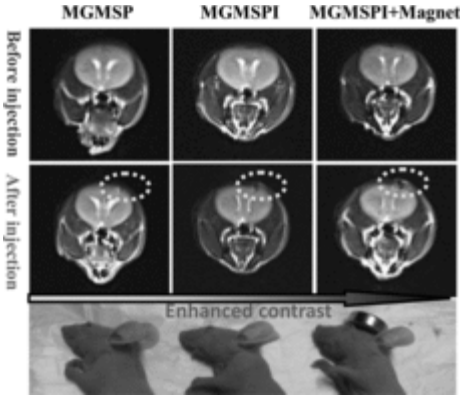

Figure 14 T2-weigted MR imaging of the glioma-bearing mice with different treatment. All the images showed that the MGMSPI drug carrier could accumulate in the tumour and image the tumour after intravenous injection. The gradually enhanced contrast illuminated the IP-mediated targeting and magnetic targeting.

PET and SPECT are nuclear medicine imaging modalities used to obtain physiological information, and are often combined with CT to provide detailed anatomical information. They have become indispensable techniques in the clinic, having spatial resolution of around 2 – 10 mm [112], but are also often used in pre-clinical evaluations. SPECT or PET radionuclides are typically added to nanoparticles employing a chelator or by covalent linkage [113]. However, this might affect the properties of the nano-carriers and result in a different pharmacokinetics and biodistribution than the native nano-systems. Zhou et al. have overcome this problem by implementing ^{64}Cu (a PET agent) in CuS nanoparticles [114]. The radiotracer has been added in the form $^{64}CuCl_2$ during the synthesis of the CuS nanoparticles and behaved therefore in the same way, providing reliable pharmacokinetics and

biodistribution data. Here, ^{64}Cu also served as the therapeutic entity allowing the combination of PTT with radionuclide therapy.

Finally, it needs to be mentioned that next to the dual therapeutic possibilities accommodated by nano-platforms, they also provide multi-imaging opportunities. This is very nicely demonstrated by Huang et al. who have designed a kind of yolk-shell structures containing gold for PTT and PAI, DOX for chemotherapy and iron oxide particles for MRI (Figure 15) [115]. Here, the magnetic properties of the iron oxide have been utilized for MRI and magnetic targeting, ensuring higher tumour accumulation of the nano-capsules.

Figure 15 An overview of the combined imaging modalities and treatments of the golden yolk-shell particles. Reproduced with permission from reference [115]. Copyright 2016 American Chemical Society.

9. Conclusions and clinical perspective

In this review, the recent developments in photochemotherapy and photoradiotherapy have been summarized, illustrating the large number of synthetic possibilities nano-carriers offer in preparing smart materials with both great cell killing potential and image guidance for optimal results. All the discussed publications suggest that the combination of phototherapies with

chemotherapy or radiotherapy leads to a much more efficient tumour killing efficiency and helps to reduce the common drawbacks of the conventional therapies. Still, there are several challenges that need to be overcome before such nano-carrier systems will be employed in the clinic. The first is related to the complexity of most of the reported systems; requiring various difficult synthesis steps and eventually resulting in highly decorated nanoparticles. In reality, nanoparticles that have reached clinical studies are rather simple, and are usually prepared by a simple one-step synthesis. Take for instance the so-called Cornell dots, which are basically silica particles having very small dimensions [116]. This controversy between clinical demands and academic approaches is often encountered and it reflects both the scientists' desire to develop fascinating chemistry and the lack of communication between clinicians and scientists. A very illustrative example is the combined use of scintillation particles with external beam radiotherapy. Low energy X-rays are nearly always employed in these studies, which are not used in therapeutic beams. Furthermore, the cost of such systems is almost never taken into account even though it will play a crucial role in translation to the clinic. Perhaps the road to clinical success is found by sacrificing some of the functionalities to increase simplicity. Besides the complicated design of some particles many of them are non-degradable and can accumulate in healthy tissue where they cause inflammations in the long run. Additionally, most of the up-conversion particles are based on rare-earth elements which might be toxic even in small quantities or cause inflammation [117]. Cell viability reported in studies dealing with up-conversion particles are carried out using coated particles. However, they fail to check the integrity of the coating and possible toxicity of such systems for periods of years, which is a realistic period of time if the particles are not cleared. Last but not least, tumour accumulation is an essential part of these combined therapies, and as long as the only way for these particles to reach sufficiently high concentrations in the tumour is by intratumoural injection their application will be very limited. If scientists develop nano-

systems that can only be administered intratumourally, it is essential to recognize the tumour types that would benefit from such an approach and perform preclinical testing on the identified models. In summary, combining photo-based therapies with chemotherapy or radiotherapy can lead to impressive tumour regression or complete elimination and deserves to be studied further, provided that the factors influencing clinical translation are taken into account. Considering the fact that the photochemotherapy and photoradiotherapy are new and blooming fields we feel confident that the above-mentioned obstacles will be surpassed in the coming years.

Abbreviation	Definition
NIR	Near-infrared
CuS	Copper sulfide
PTT	Photothermal therapy
PDT	Photodynamic therapy
ROS	Reactive oxygen species
PS	Photosensitizer
DOX	Doxorubicin
DTX	Docetaxel
CDDP	Cisplatin
PTX	Paclitaxel
DNA	Deoxyribonucleic acid
LET	Linear energy transfer
PEG	Polyethylene glycol
PGlu	Polyglutamate
SN-38	7-ethyl-10-hydroxy-campothecin
EPR	Enhanced permeability and retention
IFP	Interstitial fluid pressure
CNT	Carbon nano-tube
NGO	Nano-graphene oxide
SWCNT	Single-walled carbon nano-tube
MWCNT	Multi-walled carbon nano-tube
BBB	Blood-brain barrier
PANI	Polyaniline

AuNP	Gold nanoparticle
LSPR	Localized surface plasmon resonance
DOTA	1,4,7,10-tetraazacyclododecane-1,4,7,10-tetraacetic acid
PET	Positron emission tomography
PDA	Polydopamine
SPECT	Single photon emission computed tomography
RGD	Arginine-glycine-aspartic acid
p(NIPAM-MAA-ODA)	Poly(N-isopropylacrylamide–methacrylic acid–1,4-dioxane, octadecyl acrylate)’
PB	Prussian blue
Cy-5.5	Cyanine-5.5
MRI	Magnetic resonance imaging
PAA	Poly-acrylic acid
PAH	Poly(allylamine hydrochloride)
mPEG	Methoxy polyethylene glycol
PLGA	Poly(D,L-lactideco-glycolide)
TEM	Transmission electron microscope
PBS	Phosphate buffered saline
TPGS	D-α-tocopherol PEG 1000 succinate
QD	Quantum dot
NP	Nanoparticle
CT	Computed tomography
PAI	Photoacoustic imaging
RGD	Arginylglycylaspartic acid
HSA	Human serum albumin

SNG	Metallo-supramolecular nanogels
DH	Dextran-g-histidine
Zn-POR	Tetraphenylporphyrin zinc
Fe-TPP	Iron-tetraphenylporphyrins
PCI	Photochemical internalization
CPT	Camptothecin
HP	Hematoporphyrin
DVDMS	Sinoporphyrin sodium
ICG	Indocyanine green
TPZ	Tirapazamine
HA-CD	Per-O-methyl-b-cyclo-dextrin-grafted-hyaluronic acid
TPPS4	Tetraphenyl porphine tetrasulfonic acid
SupraPS	Supramolecular assembled photosensitizers
HAase	Hyaluronidase
NCP	Nano-scale coordination polymers
DOPA	1,2-dioleoyl-sn-glycero-3-phosphate
MPS	Mononuclear phagocyte system
UCNP	Up-conversion nanoparticle
Zn-PCN	Zn-Phtalocyanine
FA	Folic acid
DSPE-PEG	1,2-distearoyl-sn-glycero-3-phosphoethanolamine-polyethylene glycol
TEOS	Tetraethyl orthosilicate
C-60	Fullerene
Zn-Por-CA-PEG	PEGylated tetraphenylporphyrin zinc

MC540	Merocyanine 540
ZnS:Cu,Co	Copper and cobalt co-doped ZnS
TBrRh123	Tetrabromorhodamine-123
H2TPACPP	Tetra(N-propynyl-4-aminocarbonylphenyl)porphyrin
NMOF	Nanometric metal-organic frameworks
Hf	Hafnium
TCPP	Tetrakis (4-carboxyphenyl) porphyrin
PEG-b-PDPA	Poly(ethylene glycol)-block-poly(diisopropanol amino ethyl methacrylate cohydroxyl methacrylate)
BPN	Black phosphorus nanosheets
NPMOF	Nanoscale zirconium-porphyrin metal–organic framework

References

[1] *The Lancet* **2016**, 388, 1459.
[2] L. A. Torre, F. Bray, R. L. Siegel, J. Ferlay, J. Lortet-Tieulent, A. Jemal, *CA: A Cancer Journal for Clinicians* **2015**, 65, 87.
[3] a) Á. Juarranz, P. Jaén, F. Sanz-Rodríguez, J. Cuevas, S. González, *Clinical and Translational Oncology* **2008**, 10, 148; b) S. S. Lucky, K. C. Soo, Y. Zhang, *Chemical Reviews* **2015**, 115, 1990.
[4] Y. Lin, J. Zhou, Y. Cheng, L. Zhao, Y. Yang, J. Wang, *International Journal of Gynecological Cancer* **2017**, 27, 93.
[5] T. S. Lawrence, A. W. Blackstock, C. McGinn, *Seminars in Radiation Oncology* **2003**, 13, 13.
[6] a) D. Luo, K. A. Carter, D. Miranda, J. F. Lovell, *Advanced Science* **2017**, 4, 1600106; b) L. Cheng, C. Wang, L. Feng, K. Yang, Z. Liu, *Chemical Reviews* **2014**, 114, 10869.
[7] V. Shanmugam, S. Selvakumar, C.-S. Yeh, *Chemical Society Reviews* **2014**, 43, 6254.
[8] L. Xu, L. Cheng, C. Wang, R. Peng, Z. Liu, *Polymer Chemistry* **2014**, 5, 1573.
[9] N. J. Hwang S, Jung S, Song J, Doh H, Kim S, *Nanomedicine* **2014**, 9, 2003.
[10] K. Yang, S. Zhang, G. Zhang, X. Sun, S.-T. Lee, Z. Liu, *Nano Letters* **2010**, 10, 3318.
[11] J. Bai, Y. Liu, X. Jiang, *Biomaterials* **2014**, 35, 5805.
[12] L. Zou, H. Wang, B. He, L. Zeng, T. Tan, H. Cao, X. He, Z. Zhang, S. Guo, Y. Li, *Theranostics* **2016**, 6, 762.
[13] F. Chen, W. Cai, *Nanomedicine (London, England)* **2015**, 10, 1.
[14] A. N. Kharlamov, A. E. Tyurnina, V. S. Veselova, O. P. Kovtun, V. Y. Shur, J. L. Gabinsky, *Nanoscale* **2015**, 7, 8003.
[15] I. J. Macdonald, T. J. Dougherty, *Journal of Porphyrins and Phthalocyanines* **2001**, 5, 105.
[16] A. E. O'Connor, W. M. Gallagher, A. T. Byrne, *Photochemistry and Photobiology* **2009**, 85, 1053.
[17] M. C. DeRosa, R. J. Crutchley, *Coordination Chemistry Reviews* **2002**, 233-234, 351.
[18] a) C. Zhang, K. Zhao, W. Bu, D. Ni, Y. Liu, J. Feng, J. Shi, *Angewandte Chemie International Edition* **2015**, 54, 1770; b) R. Zhang, R. Xing, T. Jiao, K. Ma, C. Chen, G. Ma, X. Yan, *ACS Applied Materials & Interfaces* **2016**, 8, 13262.
[19] Y. Shi, A. Elkhabaz, F. A. Yousef Yengej, J. van den Dikkenberg, W. E. Hennink, C. F. van Nostrum, *Advanced Healthcare Materials* **2014**, 3, 2023.
[20] S. Yang, N. Li, Z. Liu, W. Sha, D. Chen, Q. Xu, J. Lu, *Nanoscale* **2014**, 6, 14903.
[21] A. M. Society, **1960**.
[22] D. Liu, F. Yang, F. Xiong, N. Gu, *Theranostics* **2016**, 6, 1306.
[23] R. Solomon, A. A. Gabizon, *Clinical Lymphoma and Myeloma* **2008**, 8, 21.
[24] D. Ersahin, I. Doddamane, D. Cheng, *Cancers* **2011**, 3, 3838.
[25] P. Nickers, I. Kunkler, P. Scalliet, *European Journal of Cancer* **1997**, 33, 1747.
[26] D. Kwatra, A. Venugopal, S. Anant, *Translational Cancer Research* **2013**, 2, 330.
[27] I. M. R. T. C. W. Group, *International Journal of Radiation Oncology • Biology • Physics* 51, 880.
[28] C.-H. Kim, Y.-S. Im, D.-H. Nam, K. Park, J.-H. Kim, J.-I. Lee, *Journal of Korean Neurosurgical Society* **2008**, 44, 358.
[29] M. Z. Ahmad, S. Akhter, G. K. Jain, M. Rahman, S. A. Pathan, F. J. Ahmad, R. K. Khar, *Expert Opinion on Drug Delivery* **2010**, 7, 927.
[30] W. B. Liechty, D. R. Kryscio, B. V. Slaughter, N. A. Peppas, *Annual review of chemical and biomolecular engineering* **2010**, 1, 149.
[31] A. Puri, K. Loomis, B. Smith, J.-H. Lee, A. Yavlovich, E. Heldman, R. Blumenthal, *Critical reviews in therapeutic drug carrier systems* **2009**, 26, 523.
[32] I. I. Slowing, J. L. Vivero-Escoto, C.-W. Wu, V. S. Y. Lin, *Advanced Drug Delivery Reviews* **2008**, 60, 1278.
[33] C. McCallion, J. Burthem, K. Rees-Unwin, A. Golovanov, A. Pluen, *European Journal of Pharmaceutics and Biopharmaceutics* **2016**, 104, 235.

[34] S. Jin, J. C. Leach, K. Ye, in *Micro and Nano Technologies in Bioanalysis: Methods and Protocols*, DOI: 10.1007/978-1-59745-483-4_34 (Eds: R. S. Foote, J. W. Lee), Humana Press, Totowa, NJ **2009**, p. 547.
[35] M. Babaei, M. Ganjalikhani, *BioImpacts : BI* **2014**, 4, 15.
[36] S. K. Nune, P. Gunda, P. K. Thallapally, Y.-Y. Lin, M. L. Forrest, C. J. Berkland, *Expert opinion on drug delivery* **2009**, 6, 1175.
[37] Y. Matsumura, *Advanced Drug Delivery Reviews* **2008**, 60, 899.
[38] H. Kobayashi, R. Watanabe, P. L. Choyke, *Theranostics* **2014**, 4, 81.
[39] a) L. Zhang, H. Su, J. Cai, D. Cheng, Y. Ma, J. Zhang, C. Zhou, S. Liu, H. Shi, Y. Zhang, C. Zhang, *ACS Nano* **2016**, 10, 10404; b) W. Zhang, Y. Li, J.-H. Sun, C.-P. Tan, L.-N. Ji, Z.-W. Mao, *Chemical Communications* **2015**, 51, 1807.
[40] T. Lammers, F. Kiessling, W. E. Hennink, G. Storm, *Journal of Controlled Release* **2012**, 161, 175.
[41] H. Kobayashi, K. Reijnders, S. English, A. T. Yordanov, D. E. Milenic, A. L. Sowers, D. Citrin, M. C. Krishna, T. A. Waldmann, J. B. Mitchell, M. W. Brechbiel, *Clinical Cancer Research* **2004**, 10, 7712.
[42] M. Caldorera-Moore, N. Guimard, L. Shi, K. Roy, *Expert Opinion on Drug Delivery* **2010**, 7, 479.
[43] a) C. Cha, S. R. Shin, N. Annabi, M. R. Dokmeci, A. Khademhosseini, *ACS nano* **2013**, 7, 2891; b) A. Bianco, K. Kostarelos, C. D. Partidos, M. Prato, *Chemical Communications* **2005**, DOI: 10.1039/B410943K571.
[44] M. Zhang, W. Wang, F. Wu, P. Yuan, C. Chi, N. Zhou, *Carbon* **2017**, 123, 70.
[45] a) L. Zhang, J. Xia, Q. Zhao, L. Liu, Z. Zhang, *Small* **2010**, 6, 537; b) H. Dong, M. Jin, Z. Liu, H. Xiong, X. Qiu, W. Zhang, Z. Guo, *Lasers in Medical Science* **2016**, 31, 1123; c) J. Song, X. Yang, O. Jacobson, L. Lin, P. Huang, G. Niu, Q. Ma, X. Chen, *ACS Nano* **2015**, 9, 9199; d) H. Chen, Z. Liu, S. Li, C. Su, X. Qiu, H. Zhong, Z. Guo, *Theranostics* **2016**, 6, 1096.
[46] Q. Zhao, X. Wang, Y. Yan, D. Wang, Y. Zhang, T. Jiang, S. Wang, *European Journal of Pharmaceutical Sciences* **2017**, 99, 66.
[47] a) A. Ruggiero, C. H. Villa, E. Bander, D. A. Rey, M. Bergkvist, C. A. Batt, K. Manova-Todorova, W. M. Deen, D. A. Scheinberg, M. R. McDevitt, *Proceedings of the National Academy of Sciences of the United States of America* **2010**, 107, 12369; b) L. Lacerda, M. Herrero, K. Venner, A. Bianco, M. Prato, K. Kostarelos, *Carbon-Nanotube Shape and Individualization Critical for Renal Excretion*, **2008**.
[48] N. S. Abadeer, C. J. Murphy, *The Journal of Physical Chemistry C* **2016**, 120, 4691.
[49] R. S. Riley, E. S. Day, *Wiley Interdisciplinary Reviews: Nanomedicine and Nanobiotechnology* **2017**, 9, e1449.
[50] a) S. Shen, H. Tang, X. Zhang, J. Ren, Z. Pang, D. Wang, H. Gao, Y. Qian, X. Jiang, W. Yang, *Biomaterials* **2013**, 34, 3150; b) D. Wang, Z. Xu, H. Yu, X. Chen, B. Feng, Z. Cui, B. Lin, Q. Yin, Z. Zhang, C. Chen, J. Wang, W. Zhang, Y. Li, *Biomaterials* **2014**, 35, 8374; c) T. Zhang, Z. Ding, H. Lin, L. Cui, C. Yang, X. Li, H. Niu, N. An, R. Tong, F. Qu, *European Journal of Inorganic Chemistry* **2015**, 2015, 2277; d) B. Cheng, H. He, T. Huang, S. S. Berr, J. He, D. Fan, J. Zhang, P. Xu, *Journal of Biomedical Nanotechnology* **2016**, 12, 435; e) Z. Zhang, C. Liu, J. Bai, C. Wu, Y. Xiao, Y. Li, J. Zheng, R. Yang, W. Tan, *ACS Applied Materials & Interfaces* **2015**, 7, 6211; f) H. Wang, R. Zhao, Y. Li, H. Liu, F. Li, Y. Zhao, G. Nie, *Nanomedicine: Nanotechnology, Biology and Medicine* **2016**, 12, 439.
[51] a) Y. Zhong, C. Wang, L. Cheng, F. Meng, Z. Zhong, Z. Liu, *Biomacromolecules* **2013**, 14, 2411; b) Y. Wang, Z. Zhang, S. Xu, F. Wang, Y. Shen, S. Huang, S. Guo, *Nanomedicine: Nanotechnology, Biology and Medicine* **2017**, 13, 1785; c) S. Parida, C. Maiti, Y. Rajesh, K. K. Dey, I. Pal, A. Parekh, R. Patra, D. Dhara, P. K. Dutta, M. Mandal, *Biochimica et Biophysica Acta (BBA) - General Subjects* **2017**, 1861, 3039; d) T. Zheng, G. G. Li, F. Zhou, R. Wu, J.-J. Zhu, H. Wang, *Advanced Materials* **2016**, 28, 8218.
[52] a) Y. Zhang, Z. Hou, Y. Ge, K. Deng, B. Liu, X. Li, Q. Li, Z. Cheng, P. a. Ma, C. Li, J. Lin, *ACS Applied Materials & Interfaces* **2015**, 7, 20696; b) S. Peng, Y. He, M. Er, Y. Sheng, Y. Gu, H. Chen, *Biomaterials Science* **2017**, 5, 475; c) G. Yang, R. Lv, F. He, F. Qu, S. Gai, S. Du, Z. Wei, P. Yang, *Nanoscale* **2015**, 7, 13747; d) W. Zhao, A. Li, C. Chen, F. Quan, L. Sun,

A. Zhang, Y. Zheng, J. Liu, *Journal of Materials Chemistry B* **2017**, DOI: 10.1039/C7TB01648D.
[53] Z. X. Zhao, Y. Z. Huang, S. G. Shi, S. H. Tang, D. H. Li, X. L. Chen, *Nanotechnology* **2014**, 25, 285701.
[54] Y. Deng, L. Huang, H. Yang, H. Ke, H. He, Z. Guo, T. Yang, A. Zhu, H. Wu, H. Chen, *Small* **2017**, 13, 1602747.
[55] a) G. Fu, W. Liu, Y. Li, Y. Jin, L. Jiang, X. Liang, S. Feng, Z. Dai, *Bioconjugate Chemistry* **2014**, 25, 1655; b) J. Li, F. Zhang, Z. Hu, W. Song, G. Li, G. Liang, J. Zhou, K. Li, Y. Cao, Z. Luo, K. Cai, *Advanced Healthcare Materials* **2017**, 6, 1700005; c) M. Wu, Q. Wang, X. Liu, J. Liu, *RSC Advances* **2015**, 5, 30970; d) W. Chen, K. Zeng, H. Liu, J. Ouyang, L. Wang, Y. Liu, H. Wang, L. Deng, Y.-N. Liu, *Advanced Functional Materials* **2017**, 27, 1605795; e) W. Tian, Y. Su, Y. Tian, S. Wang, X. Su, Y. Liu, Y. Zhang, Y. Tang, Q. Ni, W. Liu, M. Dang, C. Wang, J. Zhang, Z. Teng, G. Lu, *Advanced Science* **2017**, 4, 1600356; f) P. Xue, K. K. Y. Cheong, Y. Wu, Y. Kang, *Colloids and Surfaces B: Biointerfaces* **2015**, 125, 277.
[56] a) Q. Tian, M. Tang, Y. Sun, R. Zou, Z. Chen, M. Zhu, S. Yang, J. Wang, J. Wang, J. Hu, *Advanced Materials* **2011**, 23, 3542; b) X. Zhu, Y. Zhang, H. Huang, H. Zhang, L. Hou, Z. Zhang, *Journal of Drug Targeting* **2017**, 25, 425; c) H. Bi, Y. Dai, J. Xu, R. Lv, F. He, S. Gai, D. Yang, P. Yang, *Journal of Materials Chemistry B* **2016**, 4, 5938; d) X. Wang, Q. Zhang, L. Zou, H. Hu, M. Zhang, J. Dai, *RSC Advances* **2016**, 6, 20949.
[57] S. Goel, F. Chen, W. Cai, *Small (Weinheim an der Bergstrasse, Germany)* **2014**, 10, 631.
[58] B. Fadeel, A. E. Garcia-Bennett, *Advanced Drug Delivery Reviews* **2010**, 62, 362.
[59] X. Song, Q. Chen, Z. Liu, *Nano Research* **2015**, 8, 340.
[60] Z. Zhu, M. Su, *Nanomaterials* **2017**, 7, 160.
[61] F. Yan, W. Duan, Y. Li, H. Wu, Y. Zhou, M. Pan, H. Liu, X. Liu, H. Zheng, *Theranostics* **2016**, 6, 2337.
[62] S. Su, Y. Ding, Y. Li, Y. Wu, G. Nie, *Biomaterials* **2016**, 80, 169.
[63] M. R. Horsman, J. Overgaard, *Clinical Oncology* **2007**, 19, 418.
[64] a) M. Zhou, R. Zhang, M. Huang, W. Lu, S. Song, M. P. Melancon, M. Tian, D. Liang, C. Li, *Journal of the American Chemical Society* **2010**, 132, 15351; b) M. Zhou, Y. Chen, M. Adachi, X. Wen, B. Erwin, O. Mawlawi, S. Y. Lai, C. Li, *Biomaterials* **2015**, 57, 41.
[65] Y. Yong, X. Cheng, T. Bao, M. Zu, L. Yan, W. Yin, C. Ge, D. Wang, Z. Gu, Y. Zhao, *ACS Nano* **2015**, 9, 12451.
[66] N. Ma, Y.-W. Jiang, X. Zhang, H. Wu, J. N. Myers, P. Liu, H. Jin, N. Gu, N. He, F.-G. Wu, Z. Chen, *ACS Applied Materials & Interfaces* **2016**, 8, 28480.
[67] X. Yu, A. Li, C. Zhao, K. Yang, X. Chen, W. Li, *ACS Nano* **2017**, 11, 3990.
[68] P. Retif, S. Pinel, M. Toussaint, C. Frochot, R. Chouikrat, T. Bastogne, M. Barberi-Heyob, *Theranostics* **2015**, 5, 1030.
[69] P. Diagaradjane, A. Shetty, J. C. Wang, A. M. Elliott, J. Schwartz, S. Shentu, H. C. Park, A. Deorukhkar, R. J. Stafford, S. H. Cho, J. W. Tunnell, J. D. Hazle, S. Krishnan, *Nano Letters* **2008**, 8, 1492.
[70] X. Liu, X. Zhang, M. Zhu, G. Lin, J. Liu, Z. Zhou, X. Tian, Y. Pan, *ACS Applied Materials & Interfaces* **2017**, 9, 279.
[71] J. Du, X. Zheng, Y. Yong, J. Yu, X. Dong, C. Zhang, R. Zhou, B. Li, L. Yan, C. Chen, Z. Gu, Y. Zhao, *Nanoscale* **2017**, 9, 8229.
[72] X. Michalet, F. F. Pinaud, L. A. Bentolila, J. M. Tsay, S. Doose, J. J. Li, G. Sundaresan, A. M. Wu, S. S. Gambhir, S. Weiss, *Science (New York, N.Y.)* **2005**, 307, 538.
[73] J. Wang, X. Tan, X. Pang, L. Liu, F. Tan, N. Li, *ACS Applied Materials & Interfaces* **2016**, 8, 24331.
[74] M. Zhou, J. Zhao, M. Tian, S. Song, R. Zhang, S. Gupta, D. Tan, H. Shen, M. Ferrari, C. Li, *Nanoscale* **2015**, 7.
[75] X. Yi, K. Yang, C. Liang, X. Zhong, P. Ning, G. Song, D. Wang, C. Ge, C. Chen, Z. Chai, Z. Liu, *Advanced Functional Materials* **2015**, 25, 4689.
[76] L. Cheng, S. Shen, S. Shi, Y. Yi, X. Wang, G. Song, K. Yang, G. Liu, T. E. Barnhart, W. Cai, Z. Liu, *Advanced Functional Materials* **2016**, 26, 2185.

[77] M. Wang, G. Abbineni, A. Clevenger, C. Mao, S. Xu, *Nanomedicine: Nanotechnology, Biology and Medicine* **2011**, 7, 710.
[78] G. Chen, H. Qiu, P. N. Prasad, X. Chen, *Chemical Reviews* **2014**, 114, 5161.
[79] C. Dong, Z. Liu, S. Wang, B. Zheng, W. Guo, W. Yang, X. Gong, X. Wu, H. Wang, J. Chang, *ACS Applied Materials & Interfaces* **2016**, 8, 32688.
[80] X. Wang, G. Meng, S. Zhang, X. Liu, **2016**, 6, 29911.
[81] W. Zhang, J. Shen, H. Su, G. Mu, J.-H. Sun, C.-P. Tan, X.-J. Liang, L.-N. Ji, Z.-W. Mao, *ACS Applied Materials & Interfaces* **2016**, 8, 13332.
[82] G. Yang, H. Gong, X. Qian, P. Tan, Z. Li, T. Liu, J. Liu, Y. Li, Z. Liu, *Nano Research* **2015**, 8, 751.
[83] Y. Yang, M. Yu, H. Song, Y. Wang, C. Yu, *Nanoscale* **2015**, 7, 11894.
[84] X. Yao, X. Chen, C. He, L. Chen, X. Chen, *Journal of Materials Chemistry B* **2015**, 3, 4707.
[85] a) L.-B. Meng, W. Zhang, D. Li, Y. Li, X.-Y. Hu, L. Wang, G. Li, *Chemical Communications* **2015**, 51, 14381; b) Y. Zhang, F. Huang, C. Ren, L. Yang, J. Liu, Z. Cheng, L. Chu, J. Liu, *ACS Applied Materials & Interfaces* **2017**, 9, 13016.
[86] Q. Chen, X. Wang, C. Wang, L. Feng, Y. Li, Z. Liu, *ACS Nano* **2015**, 9, 5223.
[87] a) X. Yao, L. Chen, X. Chen, C. He, J. Zhang, X. Chen, *Macromolecular Rapid Communications* **2014**, 35, 1697; b) X. Yao, L. Chen, X. Chen, Z. Zhang, H. Zheng, C. He, J. Zhang, X. Chen, *ACS Applied Materials & Interfaces* **2014**, 6, 7816; c) X. Yao, L. Chen, X. Chen, Z. Xie, J. Ding, C. He, J. Zhang, X. Chen, *Acta Biomaterialia* **2015**, 25, 162.
[88] J. Wang, L. Liu, L. Ying, L. Chen, *European Polymer Journal* **2017**, 93, 87.
[89] a) X. Wang, X. Liu, Y. Li, P. Wang, X. Feng, Q. Liu, F. Yan, H. Zheng, *Biomaterials* **2017**, 141, 50; b) D. D. Luo, N. Li, K. A. Carter, C. Y. Lin, J. M. Geng, S. Shao, W. C. Huang, Y. L. Qin, G. E. Atilla-Gokcumen, J. F. Lovell, *Small* **2016**, 12, 3039.
[90] a) C.-L. Peng, M.-J. Shieh, M.-H. Tsai, C.-C. Chang, P.-S. Lai, *Biomaterials* **2008**, 29, 3599; b) G. Pasparakis, T. Manouras, M. Vamvakaki, P. Argitis, **2014**, 5, 3623.
[91] C. He, X. Duan, N. Guo, C. Chan, C. Poon, R. R. Weichselbaum, W. Lin, *Nature Communications* **2016**, 7, 12499.
[92] R. A. Schwendener, H. Schott, in *Liposomes: Methods and Protocols, Volume 1: Pharmaceutical Nanocarriers*, DOI: 10.1007/978-1-60327-360-2_8 (Ed: V. Weissig), Humana Press, Totowa, NJ **2010**, p. 129.
[93] M. Wehbe, A. Malhotra, M. Anantha, J. Roosendaal, A. W. Y. Leung, D. Plackett, K. Edwards, R. Gilabert-Oriol, M. B. Bally, *Journal of Controlled Release* **2017**, 252, 50.
[94] a) A. M. D. Bayona, C. M. Moore, M. Loizidou, A. J. MacRobert, J. H. Woodhams, *International Journal of Cancer* **2016**, 138, 1049; b) A. Høgset, L. Prasmickaite, P. K. Selbo, M. Hellum, B. Ø. Engesæter, A. Bonsted, K. Berg, *Advanced Drug Delivery Reviews* **2004**, 56, 95.
[95] M. B. Bally, P. Harvie, F. M. P. Wong, S. Kong, E. K. Wasan, D. L. Reimer, *Advanced Drug Delivery Reviews* **1999**, 38, 291.
[96] K. Berg, A. Weyergang, L. Prasmickaite, A. Bonsted, A. Høgset, M.-T. R. Strand, E. Wagner, P. K. Selbo, in *Photodynamic Therapy: Methods and Protocols*, DOI: 10.1007/978-1-60761-697-9_10 (Ed: C. J. Gomer), Humana Press, Totowa, NJ **2010**, p. 133.
[97] Y. Wang, Y. Xie, J. Li, Z.-H. Peng, Y. Sheinin, J. Zhou, D. Oupický, *ACS Nano* **2017**, 11, 2227.
[98] W.-H. Chen, G.-F. Luo, W.-X. Qiu, Q. Lei, L.-H. Liu, S.-B. Wang, X.-Z. Zhang, *Biomaterials* **2017**, 117, 54.
[99] C. He, X. Duan, N. Guo, C. Chan, C. Poon, R. R. Weichselbaum, W. Lin, **2016**, 7, 12499.
[100] a) M.-H. Chen, Y.-J. Jenh, S.-K. Wu, Y.-S. Chen, N. Hanagata, F.-H. Lin, *Nanoscale Research Letters* **2017**, 12, 62; b) H. Chen, G. D. Wang, Y. J. Chuang, Z. Zhen, X. Chen, P. Biddinger, Z. Hao, F. Liu, B. Shen, Z. Pan, J. Xie, *Nano Lett* **2015**, 15; c) W. Chen, J. Zhang, *J Nanosci Nanotechnol* **2006**, 6; d) S. Clement, W. Deng, E. Camilleri, B. C. Wilson, E. M. Goldys, *Sci Rep* **2016**, 6; e) Y. Liu, W. Chen, S. Wang, A. G. Joly, *Appl Phys Lett* **2008**, 92; f) L. Ma, X. Zou, B. Bui, W. Chen, K. H. Song, T. Solberg, *Applied Physics Letters* **2014**, 105, 013702; g) D. Bekah, D. Cooper, K. Kudinov, C. Hill, J. Seuntjens, S. Bradforth, J. Nadeau, *Journal of Photochemistry and Photobiology A: Chemistry* **2016**, 329, 26.

[101] J. P. Scaffidi, M. K. Gregas, B. Lauly, Y. Zhang, T. Vo-Dinh, *ACS Nano* **2011**, 5, 4679.
[102] F. Rossi, E. Bedogni, F. Bigi, T. Rimoldi, L. Cristofolini, S. Pinelli, R. Alinovi, M. Negri, S. C. Dhanabalan, G. Attolini, F. Fabbri, M. Goldoni, A. Mutti, G. Benecchi, C. Ghetti, S. Iannotta, G. Salviati, **2015**, 5, 7606.
[103] a) J. Takahashi, M. Misawa, *NanoBiotechnology* **2007**, 3, 116; b) W. Yang, P. W. Read, J. Mi, J. M. Baisden, K. A. Reardon, J. M. Larner, B. P. Helmke, K. Sheng, *International Journal of Radiation Oncology*Biology*Physics* **2008**, 72, 633.
[104] J. Liu, Y. Yang, W. Zhu, X. Yi, Z. Dong, X. Xu, M. Chen, K. Yang, G. Lu, L. Jiang, Z. Liu, *Biomaterials* **2016**, 97, 1.
[105] J. L. Su, B. Wang, K. E. Wilson, C. L. Bayer, Y.-S. Chen, S. Kim, K. A. Homan, S. Y. Emelianov, *Expert opinion on medical diagnostics* **2010**, 4, 497.
[106] H. J. Lee, Y. Liu, J. Zhao, M. Zhou, R. R. Bouchard, T. Mitcham, M. Wallace, R. J. Stafford, C. Li, S. Gupta, M. P. Melancon, *Journal of controlled release : official journal of the Controlled Release Society* **2013**, 172, 10.1016/j.jconrel.2013.07.020.
[107] J. Yao, S. Kang, J. Zhang, J. Du, Z. Zhang, M. Li, *ACS Biomaterials Science & Engineering* **2017**, DOI: 10.1021/acsbiomaterials.7b00344.
[108] a) B. Costas, *Measurement Science and Technology* **2009**, 20, 104020; b) C. G. Hadjipanayis, H. Jiang, D. W. Roberts, L. Yang, *Seminars in oncology* **2011**, 38, 109.
[109] Z. Ruan, L. Liu, W. Jiang, S. Li, Y. Wang, L. Yan, *Biomaterials Science* **2017**, 5, 313.
[110] W. Liu, Y.-M. Wang, Y.-H. Li, S.-J. Cai, X.-B. Yin, X.-W. He, Y.-K. Zhang, *Small* **2017**, 13, 1603459.
[111] Y. Wang, R. Huang, G. Liang, Z. Zhang, P. Zhang, S. Yu, J. Kong, *Small* **2014**, 10, 109.
[112] M. Bauer, O. Langer, in *Clinical Pharmacology: Current Topics and Case Studies*, DOI: 10.1007/978-3-319-27347-1_10 (Ed: M. Müller), Springer International Publishing, Cham **2016**, p. 139.
[113] K. Pant, O. Sedláček, R. A. Nadar, M. Hrubý, H. Stephan, *Advanced Healthcare Materials* **2017**, 6, 1601115.
[114] M. Zhou, Y. Chen, M. Adachi, X. Wen, B. Erwin, O. Mawlawi, S. Y. Lai, C. Li, *Biomaterials* **2015**, 57, 41.
[115] L. Huang, L. Ao, D. Hu, W. Wang, Z. Sheng, W. Su, *Chemistry of Materials* **2016**, 28, 5896.
[116] E. Phillips, O. Penate-Medina, P. B. Zanzonico, R. D. Carvajal, P. Mohan, Y. Ye, J. Humm, M. Gönen, H. Kalaigian, H. Schöder, H. W. Strauss, S. M. Larson, U. Wiesner, M. S. Bradbury, *Science translational medicine* **2014**, 6, 260ra149.
[117] R. Li, Z. Ji, C. H. Chang, D. R. Dunphy, X. Cai, H. Meng, H. Zhang, B. Sun, X. Wang, J. Dong, S. Lin, M. Wang, Y.-P. Liao, C. J. Brinker, A. Nel, T. Xia, *ACS Nano* **2014**, 8, 1771.

Bibliographies

Antonia Denkova is Assist. Professor at the department of Radiation Science and Technology at the Delft University of Technology. She received her Msc degree in Chemical and Biochemical Engineering from the same university (2003), where she subsequently obtained her PhD degree (2009). Her PhD work was related to fundamental questions on block copolymer self-assemblies. Currently, her research activities are mainly directed towards design of stable nano-carriers for radionuclide therapy.

Robin de Kruijff received her Msc degree in Applied Physics at Delft University of Technology (2013). She went on to work for the Radiation and Isotopes of Health group of the Reactor Institute Delft as researcher until she started as a PhD candidate in radiochemistry in January 2014 at the same group. Her research topic is “Alpha radionuclide therapy using polymeric nano-carriers: towards solving the recoil problem”. She has co-authored a number of publications on nano-carriers in the field of radiochemistry.

Pablo Serra-Crespo received his MSc degree in Chemical Engineering from the University of Alicante in 2010. In the same year he joined the Delft University of Technology where he obtained his PhD degree in 2014. He is now assistant professor at the same university at the Radiation Science & Technology department. His research interests include the development of new routes for the production and purification of radionuclides of medical interest.